1994-06

Inband radar cross section of phased arrays with parallel feeds

Flokas, Vassilios

Monterey, California. Naval Postgraduate School

NAVAL POSTGRADUATE SCHOOL
Monterey, California

THESIS

INBAND RADAR CROSS SECTION OF PHASED ARRAYS
WITH PARALLEL FEEDS

by

Vassilios Flokas

June 1994

Thesis Advisor: David C. Jenn

REPORT DOCUMENTATION PAGE

1a. REPORT SECURITY CLASSIFICATION **UNCLASSIFIED**	1b. RESTRICTIVE MARKINGS
2a. SECURITY CLASSIFICATION AUTHORITY	3. DISTRIBUTION/AVAILABILITY OF REPORT
2b. DECLASSIFICATION/DOWNGRADING SCHEDULE	Approved for public release; distribution is unlimited.
4. PERFORMING ORGANIZATION REPORT NUMBER(S)	5. MONITORING ORGANIZATION REPORT NUMBER(S)
6a. NAME OF PERFORMING ORGANIZATION Naval Postgraduate School 6b. OFFICE SYMBOL *(If applicable)* EC	7a. NAME OF MONITORING ORGANIZATION Naval Postgraduate School
6c. ADDRESS *(City, State, and ZIP Code)* Monterey, CA 93943-5000	7b. ADDRESS *(City, State, and ZIP Code)* Monterey, CA 93943-5000
8a. NAME OF FUNDING/SPONSORING ORGANIZATION 8b. OFFICE SYMBOL *(If applicable)*	9. PROCUREMENT INSTRUMENT IDENTIFICATION NUMBER
8c. ADDRESS *(City, State, and ZIP Code)*	10. SOURCE OF FUNDING NUMBERS Program Element No / Project No / Task No / Work Unit Accession Number

11 TITLE *(Include Security Classification)*
INBAND RADAR CROSS SECTION OF PHASED ARRAYS WITH PARALLEL FEEDS

12. PERSONAL AUTHOR(S)
Vassilios Flokas

13a. TYPE OF REPORT	13b. TIME COVERED	14. DATE OF REPORT *(year, month, day)*	15. PAGE COUNT
Master's Thesis	From To	June 1994	65

16. SUPPLEMENTARY NOTATION
The views expressed in this thesis are those of the author and do not reflect the official policy or position of the Department of Defense or the U. S. Government.

17. COSATI CODES			18. SUBJECT TERMS *(Continue on reverse if necessary and identify by block number)*
FIELD	GROUP	SUBGROUP	Scattering, radar cross section, phased arrays

19. ABSTRACT *(Continue on reverse if necessary and identify by block number)*

Approximate formulas for the inband radar cross section of arrays with parallel feeds are presented. To obtain the formulas, multiple reflections are neglected, and devices of the same type are assumed to have identical electrical performance. The approximate results were compared to the results obtained using a scattering matrix formulation. Both methods were in agreement in predicting RCS lobe positions, levels, and behavior with scanning. The advantages of the approximate method are its computational efficiency and its flexibility in handling an arbitrary number of coupler levels.

20. DISTRIBUTION/AVAILABILITY OF ABSTRACT	21. ABSTRACT SECURITY CLASSIFICATION	
W UNCLASSIFIED/UNLIMITED SAME AS REPORT DTIC USERS	Unclassified	
22a. NAME OF RESPONSIBLE INDIVIDUAL David C. Jenn	22b. TELEPHONE *(Include Area Code)* (408) 656-2254	22c. OFFICE SYMBOL EC/Jn

Approved for public release; distribution is unlimited.

Inband Radar Cross Section of Phased Arrays
With Parallel Feeds

by

Vassilios Flokas
Lieutenant J.G., Hellenic Navy
B.S. Hellenic Naval Academy , 1985

Submitted in partial fulfillment
of the requirements for the degree of

MASTER OF SCIENCE IN ELECTRICAL ENGINEERING

from the

NAVAL POSTGRADUATE SCHOOL
June 1994

Author : 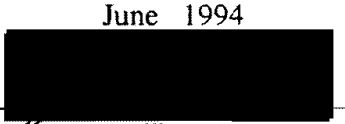
Vassilios Flokas

Approved by: 
David C. Jenn, Thesis Advisor

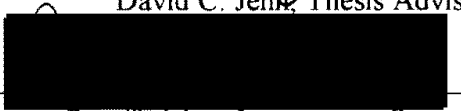
Ramakrishna Janaswamy, Second Reader


Michael A. Morgan, Chairman
Department of Electrical and Computer Engineering

ABSTRACT

Approximate formulas for the inband radar cross section of arrays with parallel feeds are presented. To obtain the formulas, multiple reflections are neglected, and devices of the same type are assumed to have identical electrical performance.

The approximate results were compared to the results obtained using a scattering matrix formulation. Both methods were in agreement in predicting RCS lobe positions, levels, and behavior with scanning. The advantages of the approximate method are its computational efficiency and its flexibility in handling an arbitrary number of coupler levels.

TABLE OF CONTENTS

I. INTRODUCTION 1

II. THEORETICAL BACKGROUND 5

A. DEFINITION OF RCS 5

B. SCATTERING FUNDAMENTALS 7

C. SCATTERING CHARACTERISTICS OF PHASED ARRAY . . . 9

D. APPROXIMATE METHOD 13

III. RCS ANALYSIS FOR THE RIGOROUS SOLUTION 28

IV. RCS OF LINEAR AND TWO-DIMENSIONAL ARRAYS 32

A. RCS DATA FOR THE APPROXIMATE SOLUTION 32

1. Linear array 32

2. Two dimensional array 40

B. RCS DATA FOR THE RIGOROUS SOLUTION 45

C. COMPARISON SUMMARY 50

V. CONCLUSIONS 51

APPENDIX A. MATLAB PROGRAM FOR LINEAR ARRAYS 52

APPENDIX B. MATLAB PROGRAM FOR PLANAR ARRAYS 54

LIST OF REFERENCES 58

INITIAL DISTRIBUTION LIST 59

I. INTRODUCTION

The design of radar-stealthy platforms has become an important engineering problem. The principles of radar stealth have been well known for several decades, but only recently have technological advances allowed practical implementation of these principles. Some examples of stealthy platforms are the SR-71 spyplane, the F-117A fighter, and the B-2 bomber. All of them have low radar cross section (RCS), low infrared (IR) emissions by control of heat sources, and low microwave emissions by using "quiet" radar and communications.

The RCS of future military platforms will be lowered significantly by the use of shaping and materials selection. Consequently, attention is now being focused on the onboard sensors in order to ensure that their signatures do not become predominant. Of particular interest are wideband phased arrays, which can possibly operate at the same frequencies as those of an illuminating threat radar. Thus a high performance array must not only meet the system antenna operating requirements (gain, sidelobe level, etc.) but also the RCS requirements. It is essential that any technique applied to minimize the radar cross section does not seriously degrade the primary operation of the antenna system.

Solid state microelectronic devices now permit integrated transmit/receive or receive-only elements to be collocated with array apertures. Self-calibrating and

adaptive "smart skin" conformal arrays are now practical. Increased efficiency, reliability, and reduced cost are the benefits of this technology. This technology makes phased arrays more appealing than other antenna types.

In characterizing and, subsequently, minimizing the RCS of phased arrays, reliable computation of scattering is crucial. It is necessary to consider both inband and out-of-band threat frequencies because the scattering characteristics of an array are distinctly different in the two frequency regions. If the incident wave is in the array's operating band, the radiating elements are well matched and threat signal can penetrate into the feed and be reflected at internal mismatches and junctions. Even for a well-matched array, there can be a large number of scattering sources that add constructively under some conditions. This effect depends on the type of feed and the devices incorporated therein. In some cases, these reflections can significantly modify the RCS.

In this thesis, the inband RCS of a phased array with a parallel (corporate) feed, as shown in Figure 1, is examined. The main objectives are:

1. to find approximate equations for the inband RCS of phased arrays with parallel feed networks,
2. to compare the approximate solution with a rigorous solution based on scattering parameters, and
3. to determine the RCS behavior for various feed parameters for both linear and two-dimensional arrays.

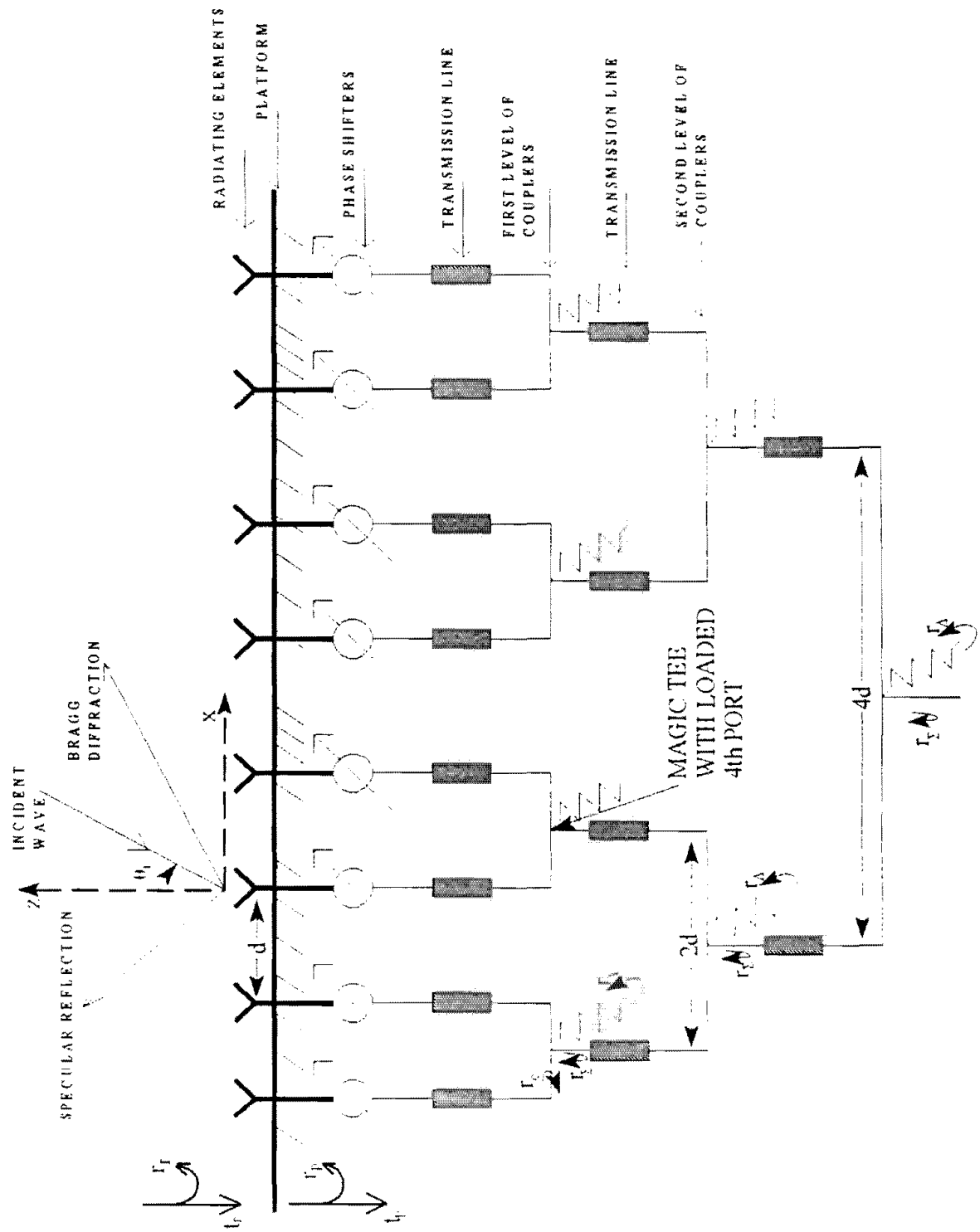

Figure 1. Typical Array Antenna with Parallel Feeds

In general, antenna scattering analysis is very difficult. Hansen [Ref. 1] describes two antenna scattering modes. The first one is the antenna or radiation mode, which is determined by the radiation properties of the antenna, and vanishes when the antenna is conjugate matched to its radiation impedance. The second is the structural mode, which is generated from currents induced on the antenna surfaces. The two modes are not easily identifiable, in particular, when the array is installed on a platform. In this thesis only the antenna mode is examined, which is the dominant RCS component for a phased array in its operating band.

Chapter II provides the theoretical background for array antenna RCS analysis and includes the derivation of the approximate formulas. It presents information about the correspondence between RCS lobes and the location of periodic scattering sources within the feed network. Chapter III describes the formation of the so-called rigorous solution. This method includes multiple reflections between devices in the feed whereas the approximate solution only considers the first reflection and neglects higher order reflections. Chapter IV deals with the comparison and analysis of results. Finally, Chapter V concludes with a discussion on the benefits, concerns, and recommendations that can be applied to the analysis of low probability of intercept radar and communications systems.

II. THEORETICAL BACKGROUND

Antennas with identical amplitude and phase patterns can differ in the way they scatter. The possible importance of this point in connection with evaluation of antennas designed to have identical patterns was first examined by R. H. Dicke [Ref. 2], who proposed "to see what can be done in the way of differentiating between a good and bad antenna on the basis of scattering."

A. DEFINITION OF RCS

The assigning of a radar cross section to a given target, whether it is an aircraft or a ship, is based on the fact that this object functions as an antenna. The back-scattering cross section may therefore be interpreted as a measure of the antenna currents excited on such an object. Radar cross section is a measure of power scattered in a given direction when a target is illuminated by an incident wave. (An older term for RCS is echo area.) Mathematically, the RCS is defined as

$$\sigma(\theta_i) = \lim_{R\to\infty} 4\pi R^2 \frac{|\underline{E}_s(\theta)|^2}{|\underline{E}_i(\theta_i)|^2} \qquad (1)$$

where R is the distance from the target to the observation point (receiver), $\underline{E}_s(\theta)$ is the scattered electric field in the direction of the receiver, and $\underline{E}_i(\theta_i)$ is the incident electric field (assumed to be a plane wave). The term monostatic means that the transmitter and receiver are co-located with respect to the target, $\theta = \theta_i$. RCS has units of square meters.

In general, RCS is a function of the angular orientation and shape of the scattering target, as well as frequency and polarization of the transmitter and receiver. Some typical values of RCS are listed in Table 1.

Table 1. RCS of Common Targets

σ in m^2	σ in dBsm	Target
0.001	-30	Insects
0.01	-20	Birds
100	20	Fighter Aircraft
1000	30	Bomber Aircraft
10000	40	Ships

The scattering characteristics for all targets fall into three natural regions. The first one is the low-frequency or Rayleigh region, defined by $kL<<1$ (L is the characteristic length of the target and $k = 2\pi/\lambda$ is the wave number). The second region is the Mie or resonance region, where kL is on the order of unity. The third is the high-frequency or optical region, where $kL>>1$. An array of length L can fall into either of the three categories depending on the threat radar's wavelength relative to the antenna's operating wavelength.

B. SCATTERING FUNDAMENTALS

Antenna scattering has been the subject of study since 1950, however there is very little published on the subject in the open literature. Until the mid 1980's, work has concentrated on the analysis of low gain antennas. Recently, high gain antennas have received attention because it is anticipated that they will be in widespread use on future low RCS platforms.

For an antenna subjected to an incident electromagnetic wave, the scattered field has traditionally been divided into two modes: the antenna mode ($\underline{E}_a$) and the structural mode ($\underline{E}_s$) [Ref. 1]. The total scattered field ($\underline{E}$) is the sum

$$\underline{E}(Z^L) = \underline{E}_s(Z_a^*) + \underline{E}_a = \underline{E}_s(Z_a^*) + \left[\frac{jZ_0}{4\lambda R_a}\underline{h}(\underline{h}\cdot\underline{E}_i)\frac{e^{-jkR}}{R}\right]r \qquad (2)$$

where

$Z_a = R_a + jX_a$ is the radiation impedance

$\underline{h}$ = effective height of the antenna

$Z_0 = 377\Omega$

$\underline{E}_i$ = incident field

The structural mode arises from currents which are induced on the antenna and the surrounding structure when the terminating load is equal to the complex conjugate of the antenna impedance. The antenna mode results when the induced current delivered to the antenna feed point is reflected and then reradiated. The antenna mode is proportional to the gain of the antenna for a given direction and a modified reflection coefficient, which is equal to

$$r = \frac{Z_L - Z_a^*}{Z_L + Z_a^*} \qquad (3)$$

where Z_L is the impedance across the antenna terminals.

When the antenna is conjugate matched, the modified reflection coefficient (r) goes to zero and the antenna mode vanishes. Usually, this is achieved when the antenna impedance has a real value and the terminals are connected to a matched transmitter and/or receiver. Consequently, there is no reflection at the junction between the antenna and the transmission line. However, Z_a for an element in an

array is dependent on the angle of arrival of the incident wave because of mutual coupling. It is practically impossible to force r to zero at every angle simultaneously.

If there is a mismatch as defined by the modified reflection coefficient, then antenna mode reflections occur. The amount of antenna mode scattering depends on the gain of the antenna in a particular direction. Thus, if the antenna does not have high gain outside of its operating band, then it will not have significant antenna mode scattering even though there is a large modified reflection coefficient.

Kahn and Kurss [Ref. 3] have demonstrated that for a large class of antennas terminated by matched receivers, the scattered power is generally greater than the absorbed power, equality being attained for minimum-scattering antennas. This result has frequently been interpreted to mean that no conjugate-matched antenna can absorb more than it scatters. This implies that gain must be lowered to reduce RCS. However, Green [Ref. 4] has shown that an antenna can absorb more than it scatters if the gain in the back direction exceeds its gain in the forward direction. This is the case for all high performance phased array antennas.

C. SCATTERING CHARACTERISTICS OF PHASED ARRAY

A single dipole provides low directivity. To increase antenna size, and hence directivity, a collection of elements can be arranged and interconnected to form an

array. The basic element can be an aperture or slot, horn, microstrip patch, spiral, or dipole depending on the application. In order to provide very directive patterns, the fields from the array elements must interfere constructively (add) in the desired directions and interfere destructively (cancel each other) in the remaining space.

The RCS of an array antenna can be decomposed into the components described in the previous section: the antenna mode and the structural mode. The relative importance of the two terms will depend primarily on the threat frequency. As shown in Figure 2 the frequency domain is separated into five bands. For a well-designed antenna, the RCS in the operating band should be low because most of the incident energy is delivered to the antenna load. However, even though the individual reflections from the antenna are small, a large array can have have tens of thousands of such sources. Thus the RCS can achieve significant levels under some conditions.

Low out-of-band	Transition band	In-band	Transition band	High out-of-band

Figure 2. Antenna Frequency Band

In this thesis, only threat signals in the operating band of the antenna will be considered. In this case, the wave penetrates into the feed network and is reflected at internal junctions and devices. The total RCS is determined by the vector sum

of the individual scattered fields that return to the aperture and reradiate. These scattering sources are depicted in Figure 1 for a parallel feed network. They include:

1. aperture, r_a
2. phase shifter inputs, r_p
3. inputs of the first level of couplers, r_c
4. loads at the sum and difference arms of the first level of couplers, r_{Σ_1}, r_{Δ_1}
5. sum and difference arm loads for higher levels of couplers, etc.

Typical sources of scattering are the following:

1. Devices that are not perfectly matched due to physical limitations (manufacturing and assembly errors, variation in the electrical properties of material, etc.)
2. Surface roughness (assembly tolerances, discontinuities, distortions, etc.)
3. Errors built into the antenna (e.g., quantization errors from subarraying)
4. Edge effects.

The inband antenna mode RCS is obtained from equations (1) and (2) and summing over all array elements

$$\sigma(\theta,\varphi) = \frac{4\pi A_e^2}{\lambda^2} \left| \sum_{n=1}^{N} \Gamma_n(\theta,\varphi) e^{j\underline{k}\cdot\underline{d}_n} \right|^2 \left| F_{norm}(\theta,\varphi) \right|^2 \qquad (4)$$

where

$\Gamma_n(\theta,\varphi)$ = total reflected signal returned to the aperture for element n when the wave is incident from the (θ,φ) direction

$\underline{k} = k(u\hat{x} + v\hat{y} + w\hat{z})$ = wave vector

$u = \sin\theta\cos\varphi$

$v = \sin\theta\sin\varphi$

$w = \cos\theta$

$\underline{d}_n$ = position vector to element n

A_e = effective area of an element = $h^2 Z_o / 4R_a$

F_{norm} = normalized element scattering pattern

To arrive at (4) identical elements have been assumed; the variation in mutual coupling near the array edges has been neglected. This allows the RCS to be separated into an array factor and an element factor, just as in the radiation case.

Evaluating (4) requires the total reflected field at each element. A rigorous solution must employ a network matrix formulation such as scattering parameters. If multiple reflections within the feed can be neglected, an approximate solution can be obtained by tracing signals through the feed and back to the aperture.

D. APPROXIMATE METHOD

In this section approximate RCS formulas are derived. The following assumptions are made:

1. All the devices of the same type are assumed to have identical electrical characteristics. That means that all the radiating elements have the same reflection coefficient r_r and the same transmission coefficient t_r. None of the elements is ideal, because each reflection coefficient r_r is not equal to zero. By the same token, all phase shifters have a reflection coefficient r_p, etc.

2. All couplers are represented by magic tees, which implies equal power splitting. (This is not a low sidelobe feed).

3. In the operating frequency band, all feed devices are well matched and therefore higher order reflections are neglected ($r << 1$).

4. Only scattering from the aperture, phase shifter inputs, coupler inputs, and the sum and difference arms of the first and second levels of couplers are considered. Couplers in higher levels of the network are assumed to be perfectly matched.

5. Lossless devices are assumed for simplicity, which implies

$$|r|^2 + |t|^2 = 1 \tag{5}$$

for a device where r is the reflection coefficient, and t is the transmission coefficient.

6. Identical aperture elements with a Lambertian scattering pattern ($\cos^2\theta$).

7. Edge effects are not included.

8. Assuming that only one scattering source dominates at any given angle, the coherent sum of the scattered signals is represented by a noncoherent sum

$$|E_1 + E_2 + \ldots + E_n|^2 \approx |E_1|^2 + |E_2|^2 + \ldots + |E_n|^2 \qquad (6)$$

where E_n is the reflected signal of the n^{th} element. Thus, the total RCS can be expressed as $\sigma = \sigma_a + \sigma_p + \sigma_{\Sigma_1} + \sigma_{\Delta_1} + \sigma_{\Sigma_2} + \sigma_{\Delta_2} + \ldots$

9. Random errors are neglected since they only contribute to an average RCS level.

Parallel feeds are suited to rectangular element arrangements, and therefore linear and rectangular array geometries will be studied. Array quantities are defined in Figure 3. Note that:

1. For the case of linear arrays, all elements are aligned along the x-axis and equally spaced, d. The z-axis is broadside to the array.

2. For the case of two dimensional planar arrays all elements are in the xy-plane, uniformly spaced with dimensions d_x and d_y, and numbers of elements N_x and N_y.

3. There is only a θ polarized incident field. (For linearly polarized elements in the xy plane, this gives rise to the $\cos^2\theta$ scattering pattern.)

4. The phase shift per element introduced by the phase shifter in Figure 1 is Δ. Furthermore, the phase shifters are reciprocal.

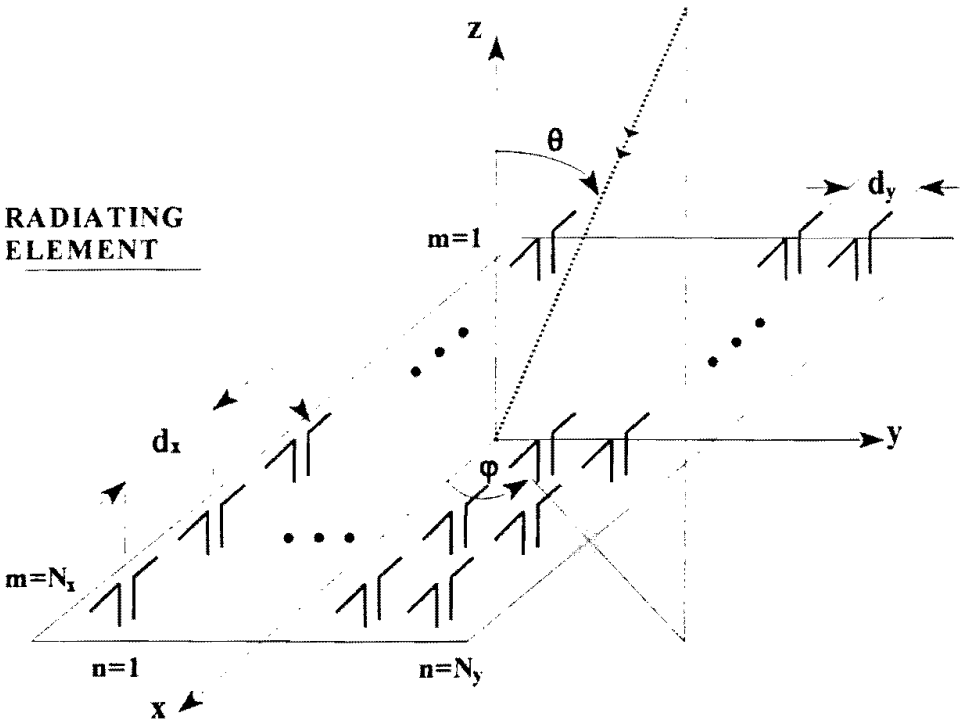

Figure 3. Two-Dimensional Array Geometry

The reflection sources for an eight element linear phased array with a parallel feed are shown in Figure 1. The incident plane wave at an angle θ arrives at each radiating element, which is the first scattering source encountered with reflection coefficient r_r. The transmitted signal, which is determined by the transmission coefficient t_r, proceeds to the phase shifter. Again, if the phase shifter is not matched to the transmission line, a reflected signal returns to the aperture, depending on the reflection coefficient r_p. A portion of this reflected field is

reflected again by the radiating element since it is assumed to be reciprocal. This is a second-order reflection, and will be neglected in the calculation of RCS. The portion of the signal not reflected at the phase shifter is transmitted to the first level of couplers, and so on.

Assuming that each phase shifter has an insertion phase, the signal that propagates through it will encounter a phase shift depending on the antenna beam scan angle θ_s. For a linear phase progression, the transmission coefficient for the phase shifter at element n is

$$t_{p_n} = t_p e^{j(n-1)\chi_0} \tag{7}$$

where $\chi_0 = kd\sin\theta_s$ for the linear array.

Figure 4 shows the first magic tee in the array with the fourth port loaded. (It can represent any three-port power divider as well.) Usually mismatches exist in both side arms, and in the sum and difference arms. The mismatches result in reflections back to the aperture, with reflection coefficients of r_c at ports 2 and 3, r_Σ at port 1, and r_Δ at port 4. The angle Δ is the signal phase at the coupler port 3 relative to the signal phase at the coupler port 2, and includes all of the insertion phases of the devices between the couplers of the first level and the aperture. It also includes any space path delay relative to the origin for the incident wave. If the phases of all reflection coefficients (except the phase shifter) are zero, then $\Delta = \alpha - \chi_0$ where $\alpha = kd\sin\theta$.

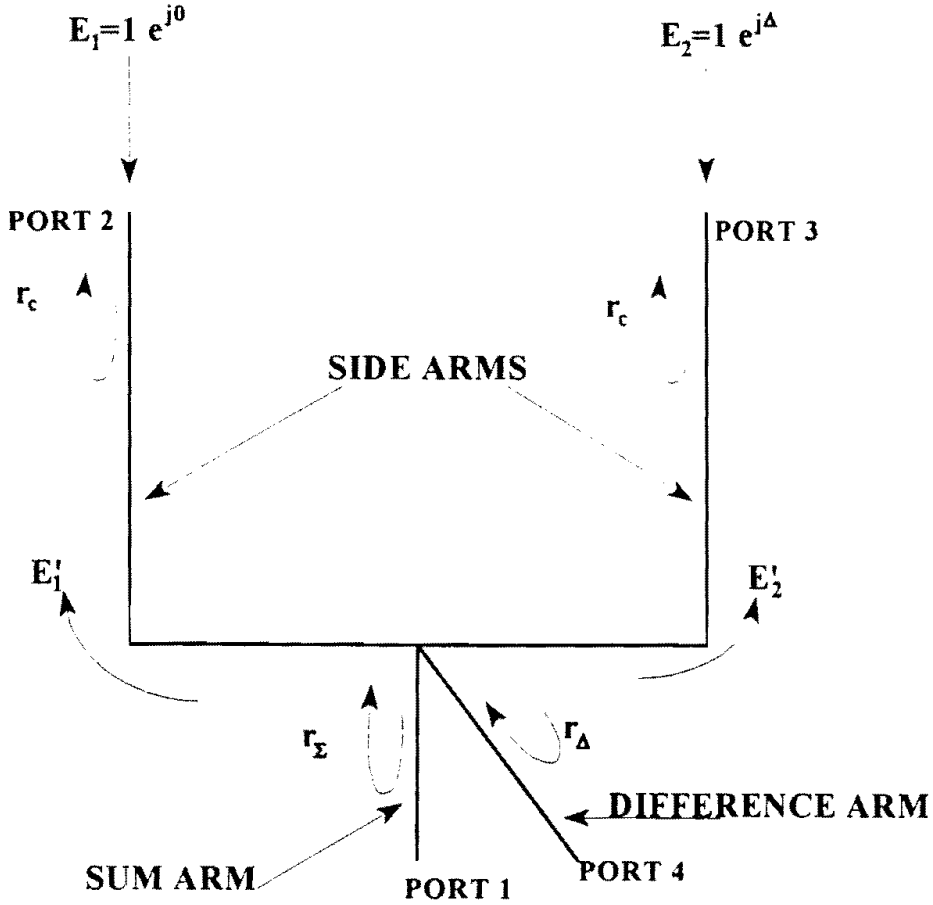

Figure 4. Reflections at the Ports of a Magic Tee.

The magic tee shown combines signals from the first two radiating elements. Similarly, the next magic tee combines signals from the third and fourth elements (2Δ at port 3 and 3Δ at port 2). The portion of the signal that enters the sum arm propagates down to the second level of couplers where some reflection occurs. with the remaining signal transmitted to the third level of couplers. and so on. For

a parallel feed network, the number of radiating elements is always of the form 2^m where m is the number of levels of couplers.

The signals reflected from the magic tee can be determined from its scattering matrix. First assume that the magic tee is perfectly matched and therefore has the following scattering matrix:

$$C = \frac{\sqrt{2}}{2}\begin{bmatrix} 0 & 1 & 1 & 0 \\ 1 & 0 & 0 & 1 \\ 1 & 0 & 0 & -1 \\ 0 & 1 & -1 & 0 \end{bmatrix}. \tag{8}$$

Referring to Figure 4, the input signals at ports 2 and 3 are E_1 and E_2 respectively. Both signals have unit amplitude but differ in phase by Δ radians. The subscripts on E refer to the element numbers to which tee's side arms are connected. In the sum arm the combined signal is

$$\begin{aligned} E_{\Sigma_1} &= E_1 + E_2 = \frac{\sqrt{2}}{2} + 1e^{j\Delta}\frac{\sqrt{2}}{2} \\ &= \sqrt{2}e^{j\frac{\Delta}{2}}\cos(\frac{\Delta}{2}). \end{aligned} \tag{9}$$

Similarly, for the difference arm the combined signal is

$$\begin{aligned} E_{\Delta_1} &= E_1 - E_2 = \frac{\sqrt{2}}{2} - \frac{\sqrt{2}}{2}e^{j\Delta} \\ &= -j\sqrt{2}e^{j\frac{\Delta}{2}}\sin(\frac{\Delta}{2}). \end{aligned} \tag{10}$$

The next magic tee in the array combines the input signals E_3 and E_4 from elements 3 and 4. Again, both signals have unit amplitude but differ in phase by Δ (because E_3 has a phase of 2Δ and E_4 has a phase of 3Δ)

$$\begin{aligned} E_{\Sigma_2} &= E_3 + E_4 = \frac{\sqrt{2}}{2} e^{j2\Delta} + \frac{\sqrt{2}}{2} e^{j3\Delta} \\ &= \sqrt{2}\, e^{j\frac{5}{2}\Delta} \cos(\frac{\Delta}{2}) , \end{aligned} \tag{11}$$

and

$$E_{\Delta_2} = E_3 - E_4 = -j\sqrt{2}\, e^{j\frac{5}{2}\Delta} \sin(\frac{\Delta}{2}) . \tag{12}$$

In general, the signals in the sum and difference arms are

$$E_{\Sigma_n} = \sqrt{2}\, e^{j\frac{\Delta}{2}} \cos\left(\frac{\Delta}{2}\right) e^{j(n-1)2\Delta} \tag{13a}$$

and

$$E_{\Delta_n} = -j\sqrt{2}\, e^{j\frac{\Delta}{2}} \sin\left(\frac{\Delta}{2}\right) e^{j(n-1)2\Delta} \tag{13b}$$

for n = 1, 2, ... N/2 .

The reflected signals from the sum and difference arms of the first level of couplers have the form

$$E'_{\Sigma_n} = E_{\Sigma_n} r_\Sigma \tag{14a}$$

and

$$E'_{\Delta_n} = E_{\Delta_n} r_\Delta \,. \tag{14b}$$

Therefore the total reflected signals returning at the side arm inputs are

$$E'_1 = E'_{\Sigma_1} S_{21} + E'_{\Delta_1} S_{24} = \left[r_\Sigma \cos\left(\frac{\Delta}{2}\right) - j r_\Delta \sin\left(\frac{\Delta}{2}\right) \right] e^{j\frac{\Delta}{2}} \,, \tag{15}$$

$$E'_2 = E'_{\Sigma_1} S_{31} + E'_{\Delta_1} S_{34} = \left[r_\Sigma \cos\left(\frac{\Delta}{2}\right) + j r_\Delta \sin\left(\frac{\Delta}{2}\right) \right] e^{j\frac{\Delta}{2}} \,, \tag{16}$$

$$E'_3 = \left[r_\Sigma \cos\left(\frac{\Delta}{2}\right) - j r_\Delta \sin\left(\frac{\Delta}{2}\right) \right] e^{j\frac{\Delta}{2}} e^{j2\Delta} \,, \tag{17}$$

$$E'_4 = \left[r_\Sigma \cos\left(\frac{\Delta}{2}\right) + j r_\Delta \sin\left(\frac{\Delta}{2}\right) \right] e^{j\frac{\Delta}{2}} e^{j2\Delta} \,. \tag{18}$$

As expected, these equations indicate that the RCS depends on the relative phases of the signals entering the side arms.

The total scattered signal due to first level of couplers is obtained by summing all reflections returned to the aperture

$$E_1^S = E_1' + E_2' + E_3' + E_4' + \ldots + E_N' . \qquad (19)$$

The phase shifter delay and path delay in the direction of the observer must be included. Summing the terms in (19) yields [Ref. 5]

$$E_1^S = r_\Sigma \cos^2\left(\frac{\Delta}{2}\right)\left[\frac{\sin(N\Delta)}{\frac{N}{2}\sin(2\Delta)}\right] - r_\Delta \sin^2\left(\frac{\Delta}{2}\right)\left[\frac{\sin(N\Delta)}{\frac{N}{2}\sin(2\Delta)}\right] . \qquad (20)$$

This can be interpreted as the sum of returns from the sum arm plus returns from the difference arms. Applying the definition of RCS gives

$$\sigma_{\Sigma_1} = \frac{4\pi A^2}{\lambda^2} r_\Sigma^2 \cos^4\left(\frac{\Delta}{2}\right)\left[\frac{\sin(N\Delta)}{\frac{N}{2}\sin(2\Delta)}\right]^2 \qquad (21a)$$

and

$$\sigma_{\Delta_1} = \frac{4\pi A^2}{\lambda^2} r_\Delta^2 \sin^4\left(\frac{\Delta}{2}\right)\left[\frac{\sin(N\Delta)}{\frac{N}{2}\sin(2\Delta)}\right]^2 . \qquad (21b)$$

The portion of the signal not reflected by the first level of couplers is transmitted down to the second level where the entire process is repeated. The total signal returned to the aperture due to reflections at the second level of couplers is

$$E_2^s = 4\sqrt{2}\cos^2\left(\frac{\Delta}{2}\right)\cdot\left[r_\Sigma\cos^2\Delta - r_\Delta\sin^2\Delta\right]\left[\frac{\sin(N\Delta)}{\sin(4\Delta)}\right]\cdot e^{j3\Delta} \quad . \tag{22}$$

Again, this is a sum of RCS contributions from the sum and difference arms,

$$\sigma_{\Sigma_2} = \frac{4\pi A^2}{\lambda^2} r_\Sigma^2 \cos^4\left(\frac{\Delta}{2}\right)\cdot\cos^4\Delta\cdot\left[\frac{\sin(N\Delta)}{\frac{N}{4}\sin(4\Delta)}\right]^2 \tag{23a}$$

$$\sigma_{\Delta_2} = \frac{4\pi A^2}{\lambda^2} r_\Delta^2 \cos^4\left(\frac{\Delta}{2}\right)\cdot\sin^4\Delta\cdot\left[\frac{\sin(N\Delta)}{\frac{N}{4}\sin(4\Delta)}\right]^2 \quad . \tag{23b}$$

The coupler RCS contribution contains three factors. The first one is $(4\pi A^2 r^2/\lambda^2)$, the RCS of a reflector of area A reduced by the reflection coefficient r^2. The squared terms in large brackets are an array factor for the couplers. Finally, the remaining factors are equivalent to an element factor for the coupler sum or difference arms.

For linearly polarized radiating elements along the x-axis and a θ-polarized incident wave, the element factor is

$$F_{norm}(\theta,\varphi) = \cos\theta \; . \tag{24}$$

This factor can be lumped with A to form a projected area. The physical area is

related to the number of elements and the spacing. Thus for a linear array

$$A = N d l \cos\theta \tag{25}$$

where

N is the number of elements

d is the spacing between elements

l is the effective height of the element.

For every RCS contribution, the first and the last factor of (4) remain the same, but the second factor is different. These are designated as array factors even though they include the subarray factors for the couplers. The array factor for the radiation element contribution is:

$$AF_r = r_r \left(\frac{\sin(N\alpha)}{N\sin(\alpha)} \right). \tag{26}$$

The array factor for the phase shifter contribution is:

$$AF_p = r_p t_r^2 \left(\frac{\sin(N\alpha)}{N\sin(\alpha)} \right). \tag{27}$$

The array factor for the side arms of the first level of couplers becomes:

$$AF_c = t_r^2 t_p^2 r_c \left(\frac{\sin(N\Delta)}{N\sin(\Delta)} \right). \tag{28}$$

The array factor for the sum arms of the first level of couplers becomes:

$$AF_{\Sigma_1} = t_r^2 t_p^2 r_\Sigma \cos^2\left(\frac{\Delta}{2}\right)\left(\frac{\sin(N\Delta)}{\frac{N}{2}\sin(2\Delta)}\right) \tag{29}$$

which occurs in (21a). The array factor for the difference arms of the first level of couplers becomes:

$$AF_{\Delta_1} = t_r^2 t_p^2 r_\Delta \sin^2\left(\frac{\Delta}{2}\right)\left(\frac{\sin(N\Delta)}{\frac{N}{2}\sin(2\Delta)}\right) \tag{30}$$

which also occurs in (21b).

The array factor for the sum arms of the second level of couplers becomes:

$$AF_{\Sigma_2} = t_r^2 t_p^2 r_\Sigma \cos^2\left(\frac{\Delta}{2}\right)\cos^2(\Delta)\left(\frac{\sin(N\Delta)}{\frac{N}{4}\sin(4\Delta)}\right) \tag{31}$$

which is related to (23a). The array factor for the difference arms of the second level of couplers becomes:

$$AF_{\Delta_2} = t_r^2 t_p^2 r_\Delta \cos^2\left(\frac{\Delta}{2}\right)\sin^2(\Delta)\left(\frac{\sin(N\Delta)}{\frac{N}{4}\sin(4\Delta)}\right) \tag{32}$$

which is also related to (23b). By combining (4) and (6), the total monostatic

inband antenna mode RCS is

$$\sigma = \frac{4\pi A^2}{\lambda^2}(AF_r^2 + AF_p^2 + AF_c^2 + AF_{\Sigma_1}^2 + AF_{\Delta_1}^2 + AF_{\Sigma_2}^2 + AF_{\Delta_2}^2). \quad \textbf{(33)}$$

Consider a of two-dimensional planar array in the xy-plane with a rectangular grid as shown in Figure 3. The array has N_x by N_y elements spaced d_x by d_y. Parallel feeds are used to combine signals for elements along the x-axis. Thus the results for the linear array can be applied directly to the two-dimensional array by choosing Δ properly and multiplying all terms by a y-direction array factor. If θ_s and φ_s are the scanned antenna beam angles, then let

$$\chi_{0x} = kd_x \sin\theta_s \cos\varphi_s \quad \textbf{(34a)}$$

and

$$\chi_{0y} = kd_y \sin\theta_s \sin\varphi_s \quad \textbf{(34b)}$$

be the interelement phases to scan the antenna beam. Now Δ in the linear array formulas is replaced by ζ_x where

$$\zeta_x = kd_x u - \chi_{0x}. \quad \textbf{(35)}$$

All scattering terms for the linear array must be multiplied by an array factor for the y-dimension. For scattering sources ahead of the phase shifters

$$AF_y = \left(\frac{\sin(N_y k d_y v)}{N_y \sin(k d_y v)}\right), \tag{36}$$

and for scattering sources behind the phase shifters

$$AF_y = \left(\frac{\sin(N_y \zeta_y)}{N_y \sin(\zeta_y)}\right), \tag{37}$$

where

$$\zeta_y = k d_y v - \chi_{0y} . \tag{38}$$

Thus, for a two-dimensional array equations (26) through (32) become

$$AF_r = r_r \left(\frac{\sin(N_x k d_x u)}{N_x \sin(k d_x u)}\right)\left(\frac{\sin(N_y k d_y v)}{N_y \sin(k d_y v)}\right), \tag{39}$$

$$AF_p = r_p t_r^2 \left(\frac{\sin(N_x k d_x u)}{N_x \sin(k d_x u)}\right)\left(\frac{\sin(N_y k d_y v)}{N_y \sin(k d_y v)}\right), \tag{40}$$

$$AF_c = t_r^2 t_p^2 r_c \left(\frac{\sin(N_x \zeta_x)}{N_x \sin(\zeta_x)}\right)\left(\frac{\sin(N_y \zeta_y)}{N_y \sin(\zeta_y)}\right), \tag{41}$$

$$AF_{\Sigma_1} = t_r^2 t_p^2 r_\Sigma \cos^2\left(\frac{\zeta_x}{2}\right)\left(\frac{\sin(N_x \zeta_x)}{\frac{N_x}{2}\sin(2\zeta_x)}\right)\left(\frac{\sin(N_y \zeta_y)}{N_y \sin(\zeta_y)}\right), \tag{42}$$

$$AF_{\Delta_1} = t_r^2 t_p^2 r_\Delta \sin^2\left(\frac{\zeta_x}{2}\right)\left(\frac{\sin(N_x \zeta_x)}{\frac{N_x}{2}\sin(2\zeta_x)}\right)\left(\frac{\sin(N_y \zeta_y)}{N_y \sin(\zeta_y)}\right), \quad (43)$$

$$AF_{\Sigma_2} = t_r^2 t_p^2 r_\Sigma \cos^2\left(\frac{\zeta_x}{2}\right)\cos^2(\zeta_x)\left(\frac{\sin(N_x \zeta_x)}{\frac{N_x}{4}\sin(4\zeta_x)}\right)\left(\frac{\sin(N_y \zeta_y)}{N_y \sin(\zeta_y)}\right), \quad (44)$$

$$AF_{\Delta_2} = t_r^2 t_p^2 r_\Delta \cos^2\left(\frac{\zeta_x}{2}\right)\sin^2(\zeta_x)\left(\frac{\sin(N_x \zeta_x)}{\frac{N_x}{4}\sin(4\zeta_x)}\right)\left(\frac{\sin(N_y \zeta_y)}{N_y \sin(\zeta_y)}\right). \quad (45)$$

Finally, the total RCS is

$$\sigma = \frac{4\pi A^2}{\lambda^2}\left(AF_r^2 + AF_p^2 + AF_c^2 + AF_{\Sigma_1}^2 + AF_{\Delta_1}^2 + AF_{\Sigma_2}^2 + AF_{\Delta_2}^2\right) \quad (46)$$

where

$$A = N_x N_y d_x d_y \cos\theta \,. \quad (47)$$

III. RCS ANALYSIS FOR THE RIGOROUS SOLUTION

In the approximate method, the higher order reflections are neglected because they vary as r^2, r^3, etc., where $r << 1$. A rigorous solution based on a scattering matrix formulation contains the effects of multiple reflections. Furthermore, it is possible to combine scattering matrices with the method of moments to include interactions between the feed and aperture as well as reflections inside the feed. This method solves the problem rigorously by obtaining an antenna impedance matrix that describes the electrical characteristics of the antenna surfaces and feed network. The method of moments (MM) impedance matrix is combined with the feed scattering matrix and continuity equations that relate the MM expansion coefficients to the feed signals as described in [Ref. 6].

In this thesis a variation of the rigorous method in [Ref. 6] is used, where the radiating element is represented by a simple two-port device with reflection coefficient r_r. This eliminates the method of moments portion of the antenna matrix in the rigorous solution of [Ref. 6], and the problem reduces to a pure scattering matrix one. This allows direct comparison of the rigorous solution with the approximate solution, because the radiating elements are modelled the same.

A typical scattering matrix equivalent network with eight elements is shown in Figure 5. If only two levels of couplers are modelled, then only a four-element array need be considered. Reflections from the third level of couplers are zero and therefore adjacent four-element subarrays are decoupled. The four-element array problem can be solved by the scattering matrix formulation in [Ref. 6].

In the rigorous method, the number of radiating elements is assumed to be a multiple of 4. The incident plane wave field incident on element i :

$$S_i = e^{jkdu(i-1)}, \quad i = 1, 2, ..., N . \tag{48}$$

The N elements of the array can be divided into N/4 subarrays as shown in Figure 6, where the a coefficients are used to obtain the scattered field E^s

$$\begin{aligned} E^s &= \sum_{n=1}^{N} a_n e^{jkdu(n-1)} \\ &= \sum_{n=1}^{N/4} e^{j2kdu(n-1)4} \left[\sum_{i=1}^{4} a_i e^{jkdu(i-1)4} \right]. \end{aligned} \tag{49}$$

Equation (49) has been obtained using the fact that the four-element subarrays are decoupled

$$\begin{aligned} a_1 &= a_5 = a_9 = ... \\ a_2 &= a_6 = a_{10} = ... \\ a_3 &= a_7 = a_{11} = ... \\ a_4 &= a_8 = a_{12} = ... \end{aligned} \tag{50}$$

The total RCS is obtained from (1).

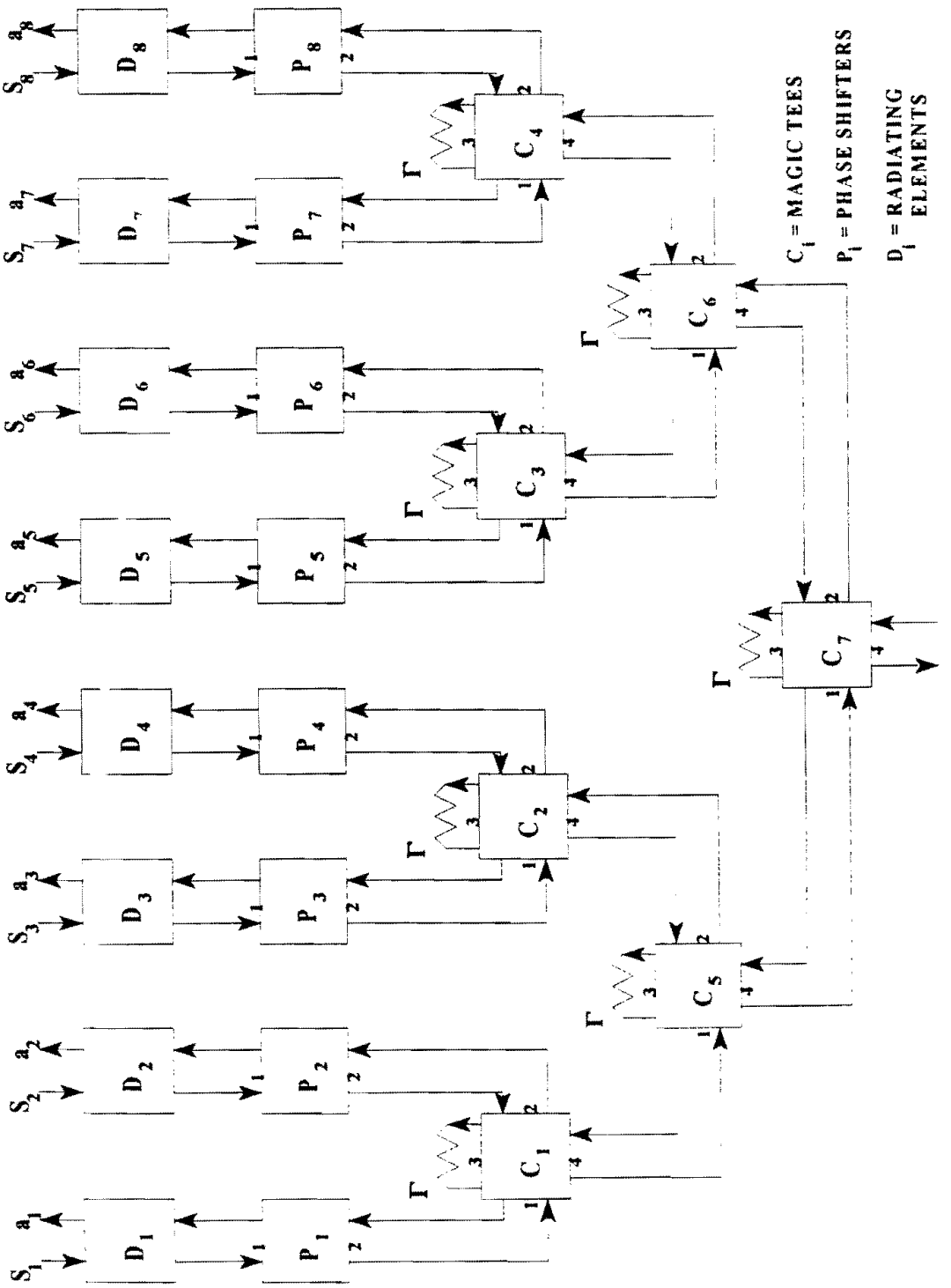

Figure 5. Typical Linear Array with N Elements Divided into N/4 Subarrays.

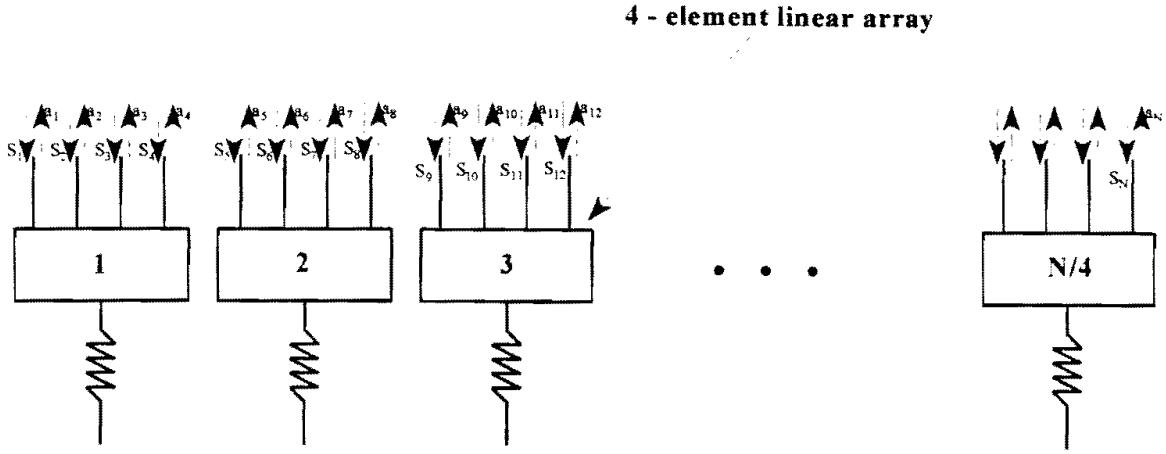

Figure 6. Scattering Matrix Equivalent Network when the Radiating Element Match is Constant with Angle

For each four-element subarray, there are eight 2-port devices (four radiating elements plus four phase shifters) that yield 16 equations, and three 4-port devices (two magic tees in the first level plus one magic tee in the second level) that yield 12 equations. There is a total of 28 equations and 28 unknowns (28 *a*'s) for the four 4-element subarray.

The important characteristics of the rigorous method are the following:

1. Interactions between all devices in the feed and radiating elements are included;

2. The transmission line phase between devices is included. Thus the effect of changing line lengths can be modelled.

IV. RCS OF LINEAR AND TWO-DIMENSIONAL ARRAYS

In order to simplify the analysis and reduce the demand for computer time, only linear arrays have been examined using the rigorous method. Thus a comparison of the two methods is only given for linear arrays. RCS contour plots for two-dimensional arrays were also obtained to illustrate RCS behavior with beam scanning. The MATLAB programs are included in the Appendices.

A. RCS DATA FOR THE APPROXIMATE SOLUTION

1. Linear array

For the approximate method, RCS pattern data for linear arrays was computed. The linear array program computes the RCS per squared wavelength in dB for any monostatic angle θ, number of radiating elements N, and scanned angle θ_s. The contributions from each scattering source can be broken out individually if desired.

The inband RCS of linear arrays with 16, 64, and 128 elements for $\theta_s = 0$ degrees (no scanning) is shown in Figures 7 through 9. All reflection coefficients for feed devices and the radiating elements are equal to 0.2

$$r_r = r_p = r_c = r_\Sigma = r_\Delta = 0.2 \quad .$$

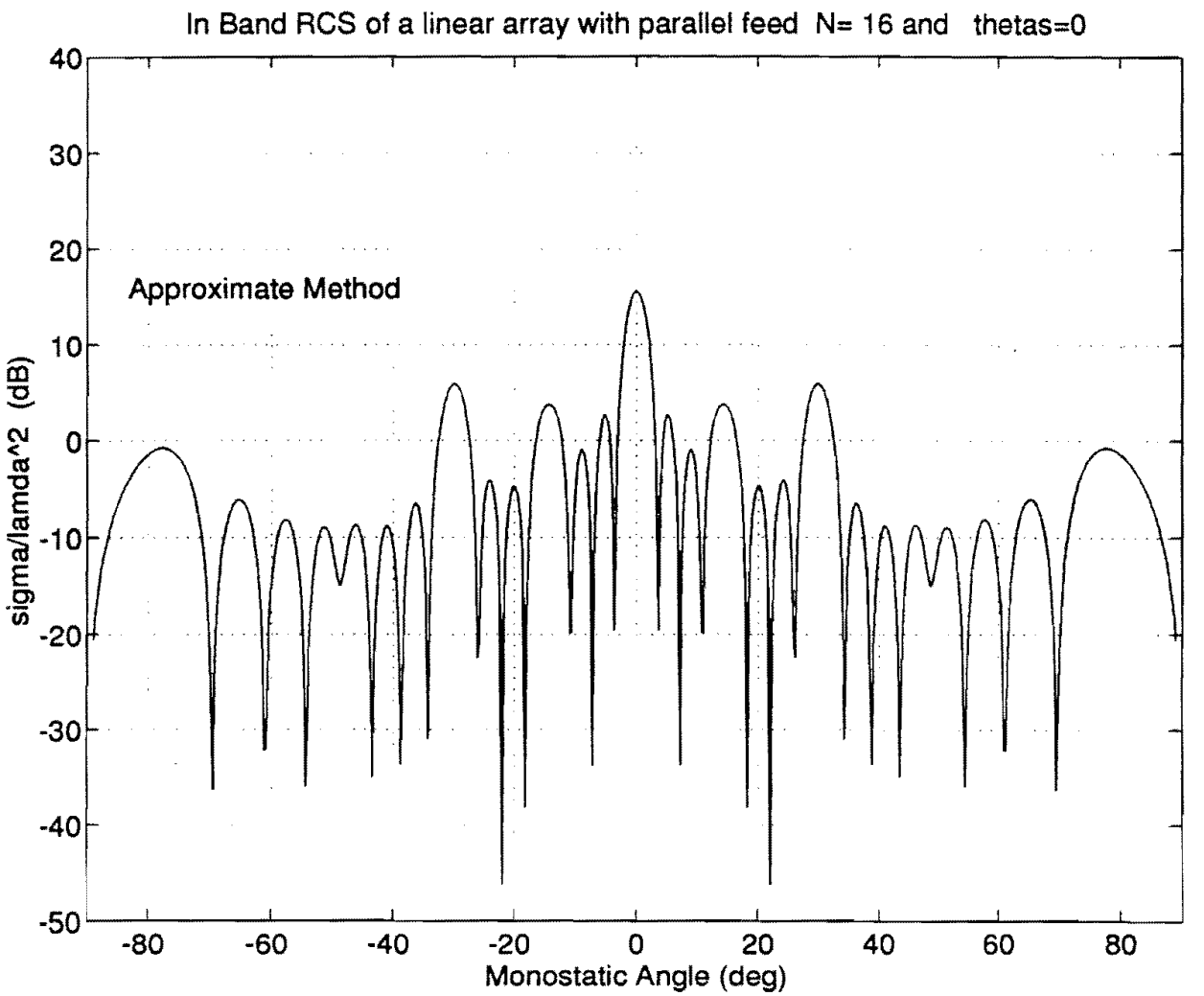

Figure 7. Inband RCS of a Linear Array with a Parallel Feed for N=16, $\theta_s = 0°$ (Approximate Method).

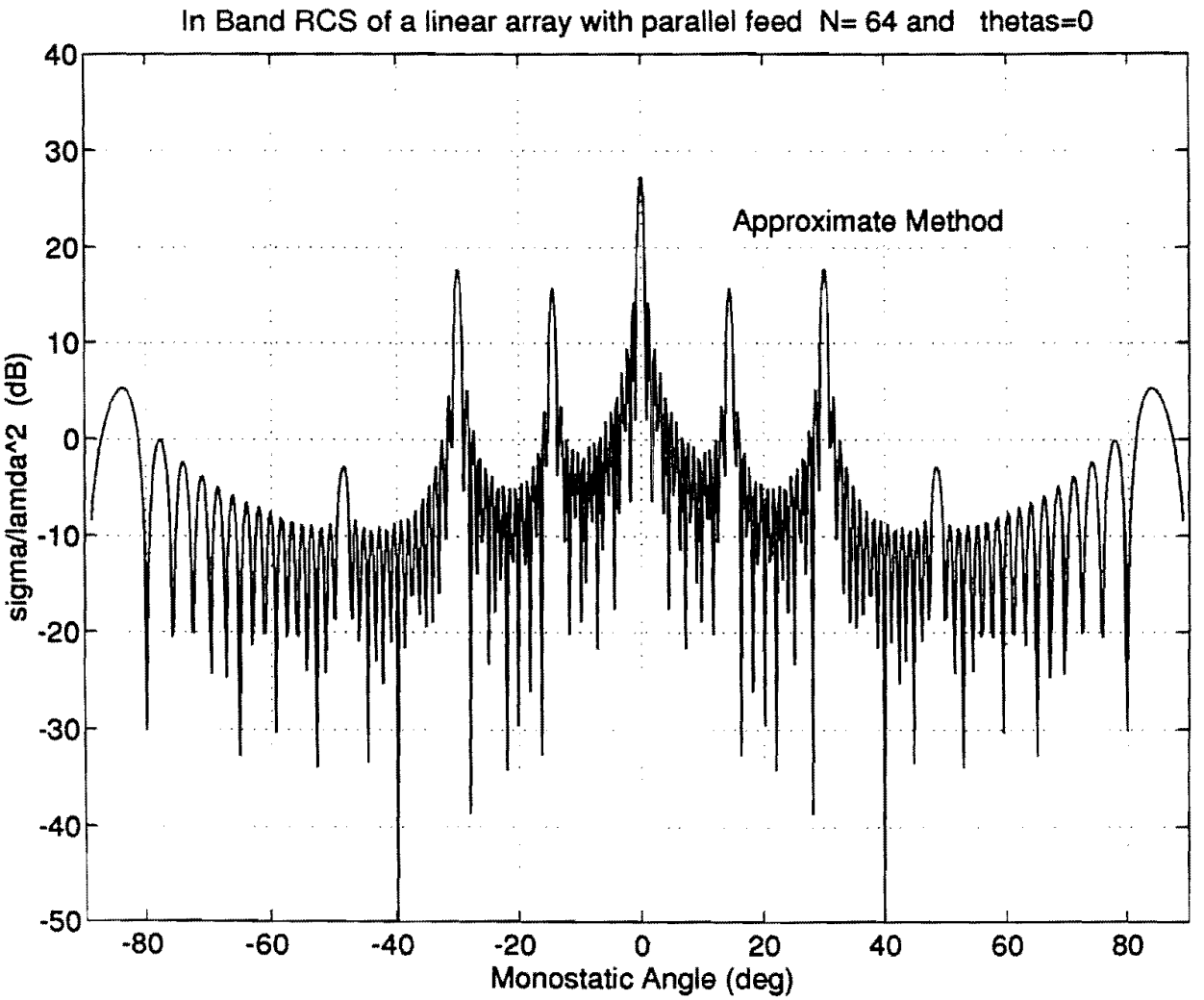

Figure 8. Inband RCS of a Linear Array with a Parallel Feed for N=64, $\theta_s = 0°$ (Approximate Method).

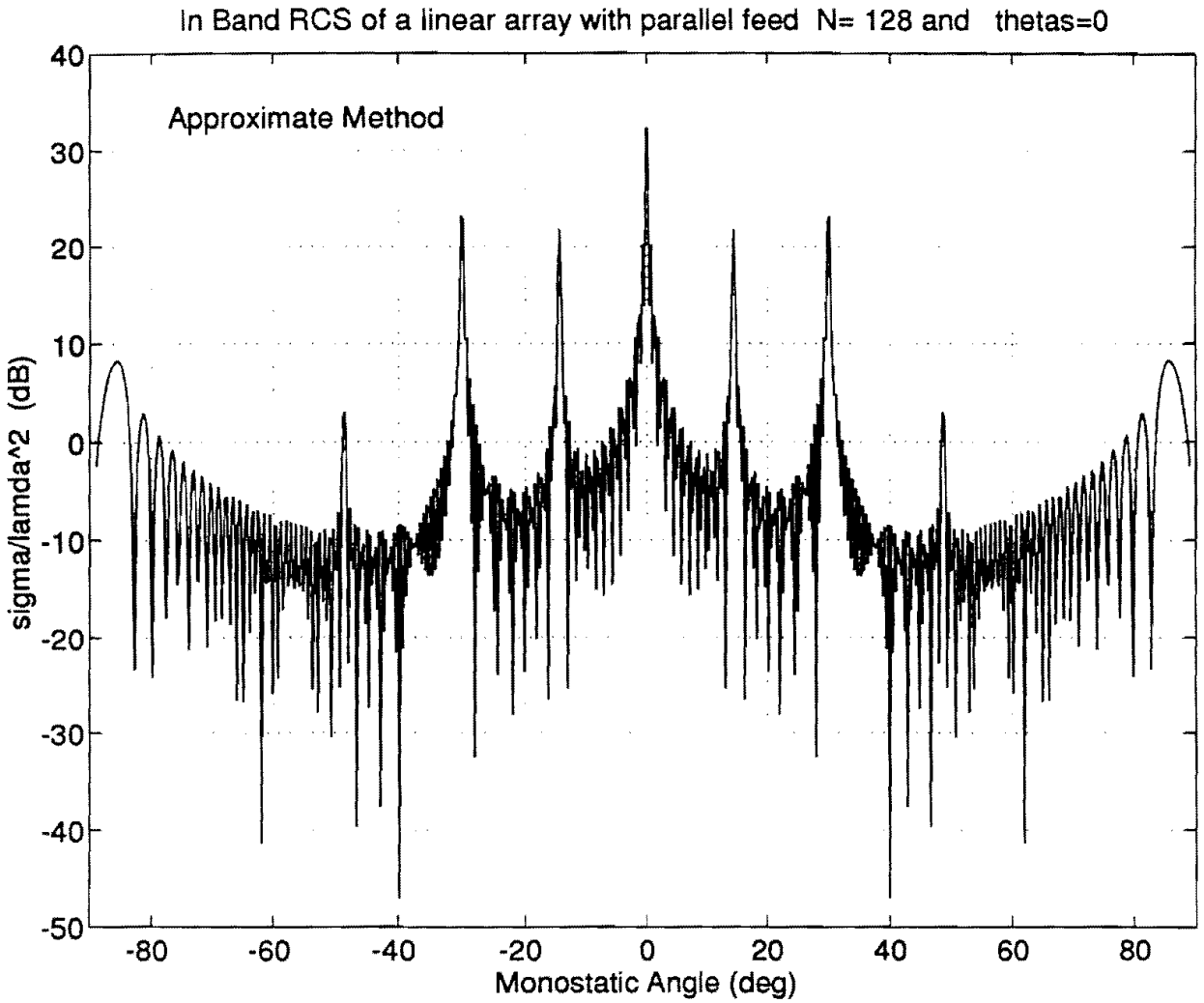

Figure 9. Inband RCS of a Linear Array with a Parallel Feed for N=128, $\theta_s = 0°$ (Approximate Method).

For all linear array calculations the spacing is $d = \lambda/2$ and the effective height (or length) of the elements in the y direction is $l = \lambda/2$.

Referring to the figures, note that the number of major lobes (spikes) is the same in all cases. For a small number of elements (e.g., N = 16) the lobes are not as well defined because they are broader and lower. The RCS contributions from first and second levels of couplers are shown in Figures 10 and 11, respectively. The lobe spacing in the RCS pattern for the first level of couplers is determined by the physical spacing of the couplers ($2d$). This can be generalized for higher levels also. For instance, the effective spacing of the second level of couplers is $4d$. Therefore, as more levels of couplers are added to the feed, more lobes appear between already existing lobes.

Figure 12 illustrates the effect of beam scanning. Assuming that the phase shifters are reciprocal devices, the lobes associated with mismatches behind the phase shifters scan with the antenna beam because of the factor χ_0 . The large lobe, at θ = 45 degrees in Figure 12 is due to in-phase addition of the scattered signals passing through the phase shifters, as expected. Note that the specular lobe at θ = 0 degrees does not scan. The high lobes near $\pm$ 85° are due to Bragg diffraction (the RCS equivalent of grating lobes).

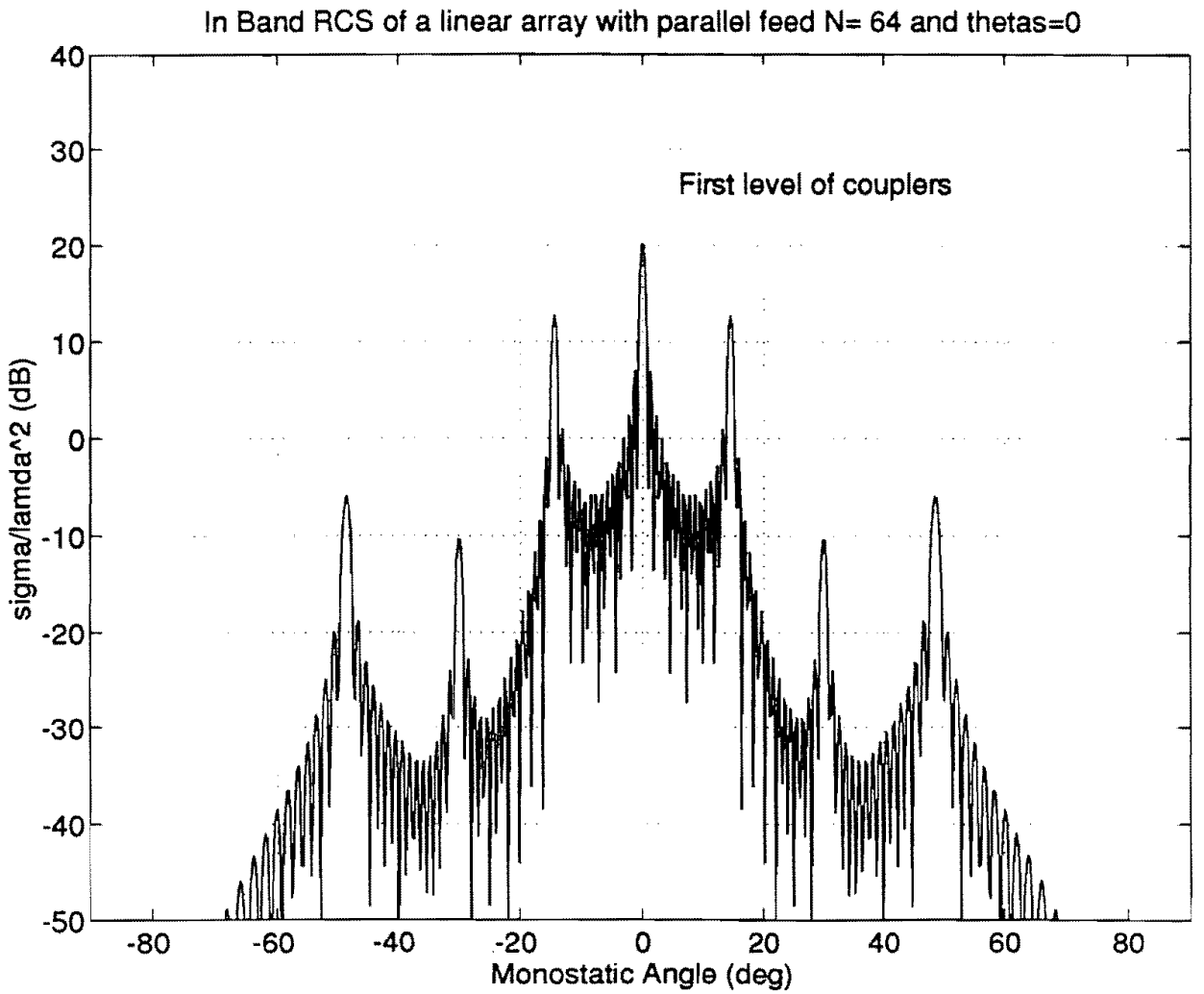

Figure 10. Contribution from First Level of Couplers.

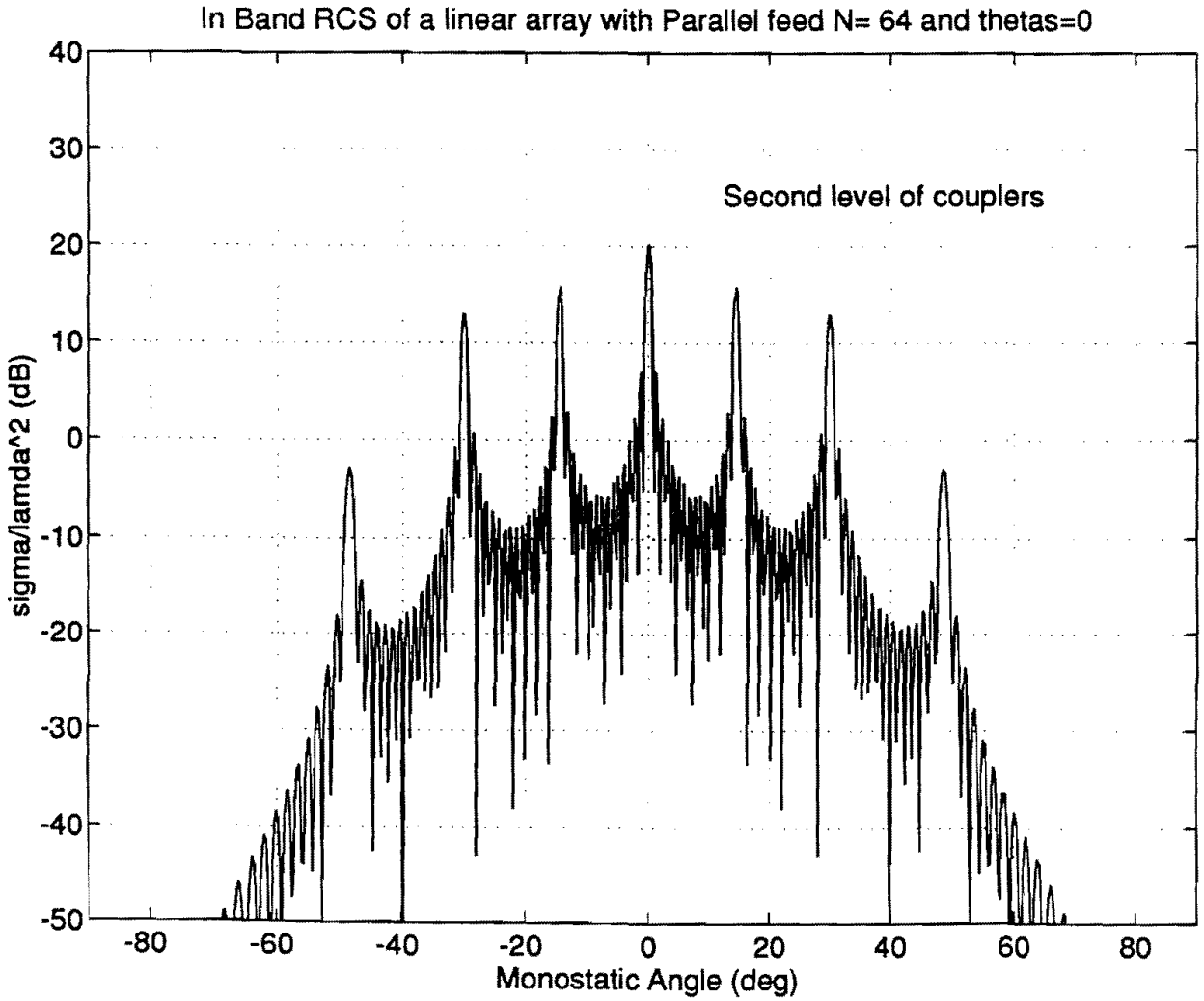

Figure 11. Contribution from Second Level of Couplers.

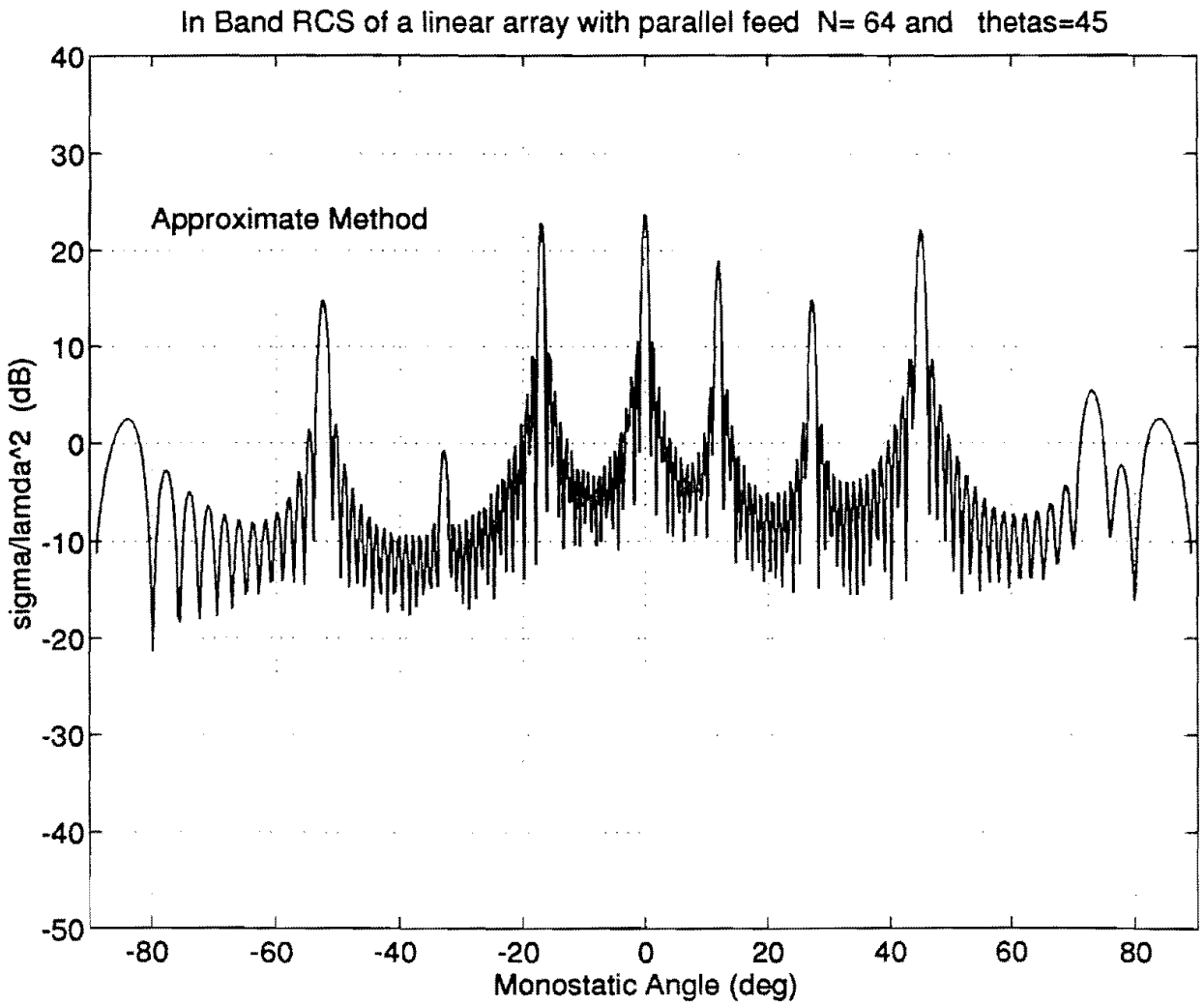

Figure 12. Inband RCS of a Linear Scanning Array with a Parallel Feed for N = 64, $\theta_s = 45°$ (Approximate Method).

2. Two dimensional array

A second MATLAB program, which is shown in Appendix B, was used to generate contour plots of inband RCS for two-dimensional arrays. For simplicity, only square arrays are examined ($N_x = N_y$ and $d_x = d_y = \lambda/2$) for a specified scan angle (θ_s, φ_s). Again it is assumed that all reflection coefficients are 0.2. RCS contours are shown in Figures 13 through 16. They are plotted in direction cosine space (u and v) and the contours enclose spatial regions of RCS above a specified level. This level is chosen to be 10 dB when $N_x = N_y = 16$. and 20 dB when $N_x = N_y = 64$ elements.

The only difference between the arrays of Figures 13 and 14 is the number of elements: 16 by 16 versus 64 by 64. Both plots are symmetric about the horizontal axis at $v = 0$. High RCS is present along the principal planes of the array and then drops off away from these axes because of the separable product in the array factors. It can be seen that the lobes are narrower and higher as the number of elements increase. The specular lobe appears at the center of each plot.

Figures 15 and 16 show the RCS of scanned arrays. The first one has $\theta_s = 45$ degrees and $\varphi_s = 0$ degrees, and the second $\theta_s = 45$ degrees and $\varphi_s = 45$ degrees. Both plots are symmetric around the axis $v = 0$. As in the linear array case, the lobes originating from reflections behind the phase shifters scan along with the antenna beam.

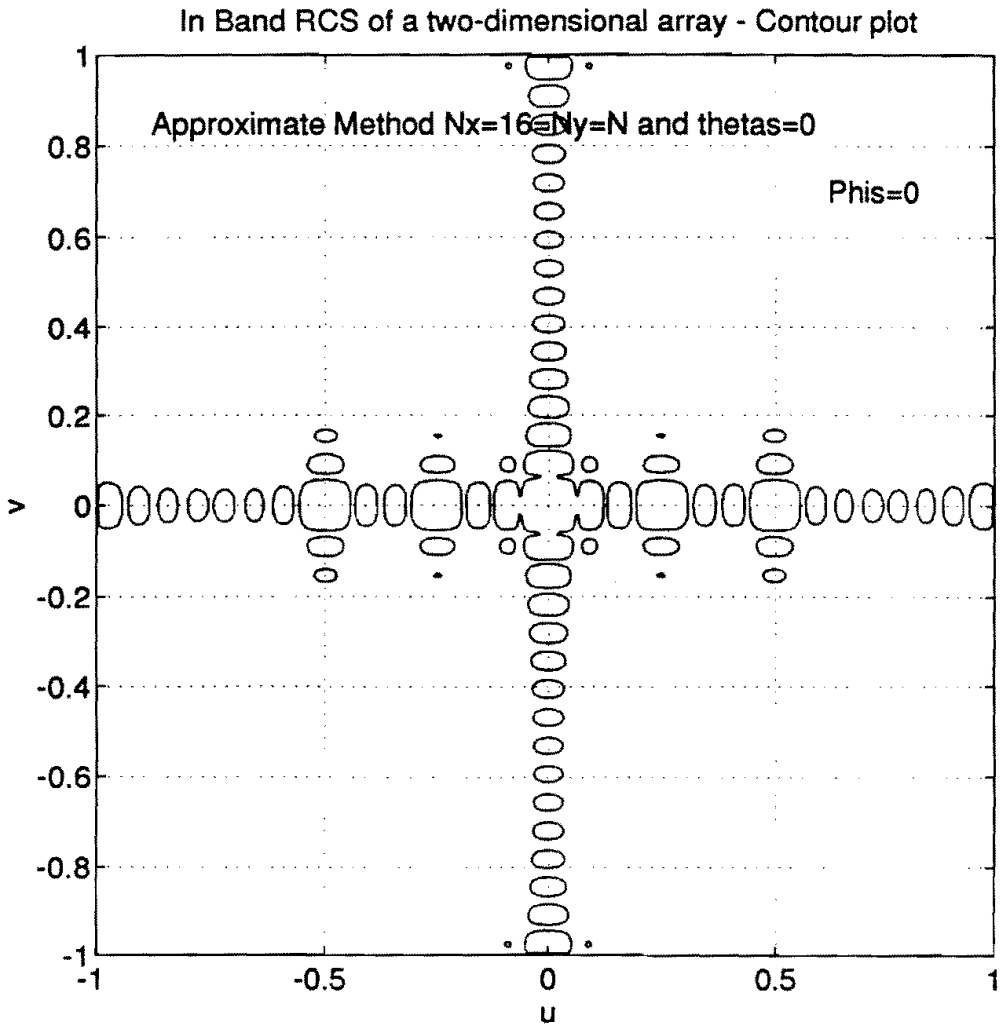

Figure 13. Inband RCS of a Two-Dimensional Array with a Parallel Feed for $N_x = N_y = 16$, $\theta_s = 0°$, $\varphi_s = 0°$. Contour Plot at 10 dB Level (Approximate Method).

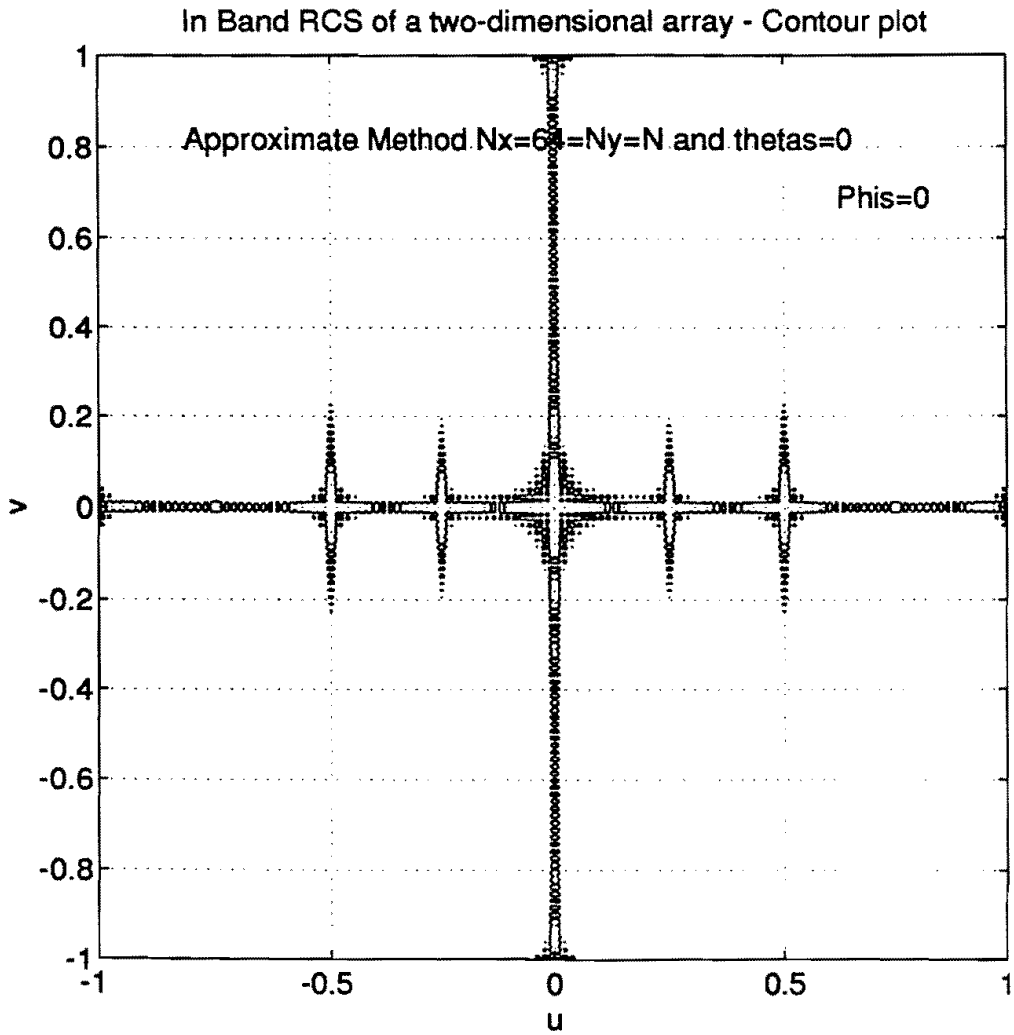

Figure 14. Inband RCS of a Two-Dimensional Array with a Parallel Feed for $N_x = N_y = 64$, $\theta_s = 0°$, $\varphi_s = 0°$. Contour Plot at 20 dB Level (Approximate Method).

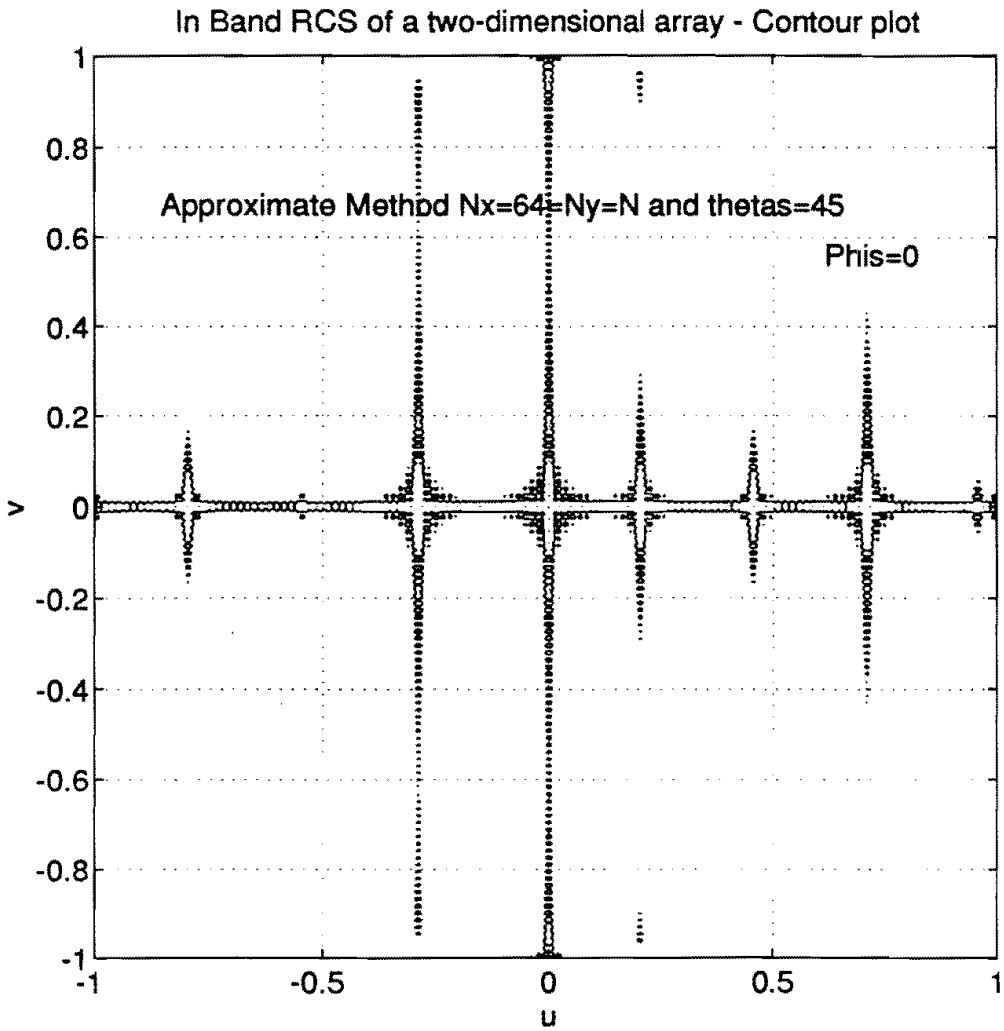

Figure 15. Inband RCS of a Two-Dimensional Array with a Parallel Feed for $N_x = N_y = 64$, $\theta_s = 45°$, $\varphi_s = 0°$. Contour Plot at 20 dB Level (Approximate Method).

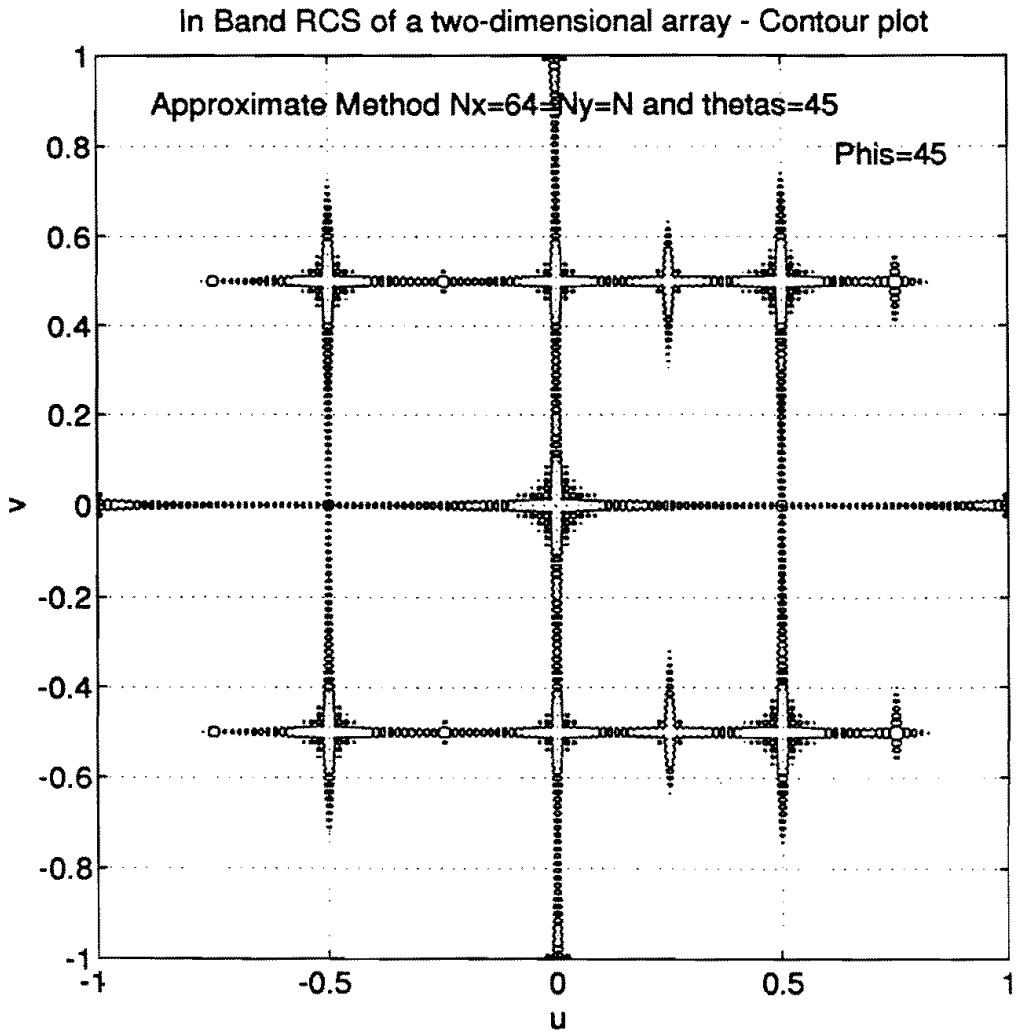

Figure 16. Inband RCS of a Two-Dimensional Array with a Parallel Feed for $N_x = N_y = 64$, $\theta_s = 45°$, $\varphi_s = 45°$. Contour Plot at 20 dB Level (Approximate Method).

B. RCS DATA FOR THE RIGOROUS SOLUTION

For the rigorous method, pattern plots of the RCS of linear arrays are obtained by using the FORTRAN program developed in [Ref. 6]. This program computes the RCS per squared wavelength in dB for any monostatic angle θ. Array parameters include the number of radiating elements N (N has to be a multiple of 8), scan angle θ_s , and electrical path length between devices ψ_0 (in radians). The output is written to MATLAB files that can be used to plot the RCS patterns.

Figure 17 shows the RCS values of a linear array for N = 64 with no scanning (θ_s = 0) and path lengths of ψ_0 = 0 radians. As in the approximate method, the specular lobe at θ = 0, coupler lobes, and Bragg lobes at θ = ±85 degrees are evident. The same array is examined in Figures 18 and 19 with ψ_0 = $\pi/4$ and $\pi/2$, respectively. A comparison of Figures 17 through 19 shows that the lobes have the same position but differ in amplitude. Specifically, for $\psi_0 = \pi/4$ the specular and coupler lobes have bigger amplitude than for ψ_0 = 0. However, for $\psi_0 = \pi/4$, the Bragg lobes have smaller amplitude than for ψ_0 = 0. The variation is due to the beating of mismatches in the feed. The addition or cancellation depends on the line lengths connecting the devices, ψ_0. This effect becomes more complicated as the beam is scanned (Figure 20). Some lobes may disappear at some scan angles because the phase shifters introduce a shift that cause complete

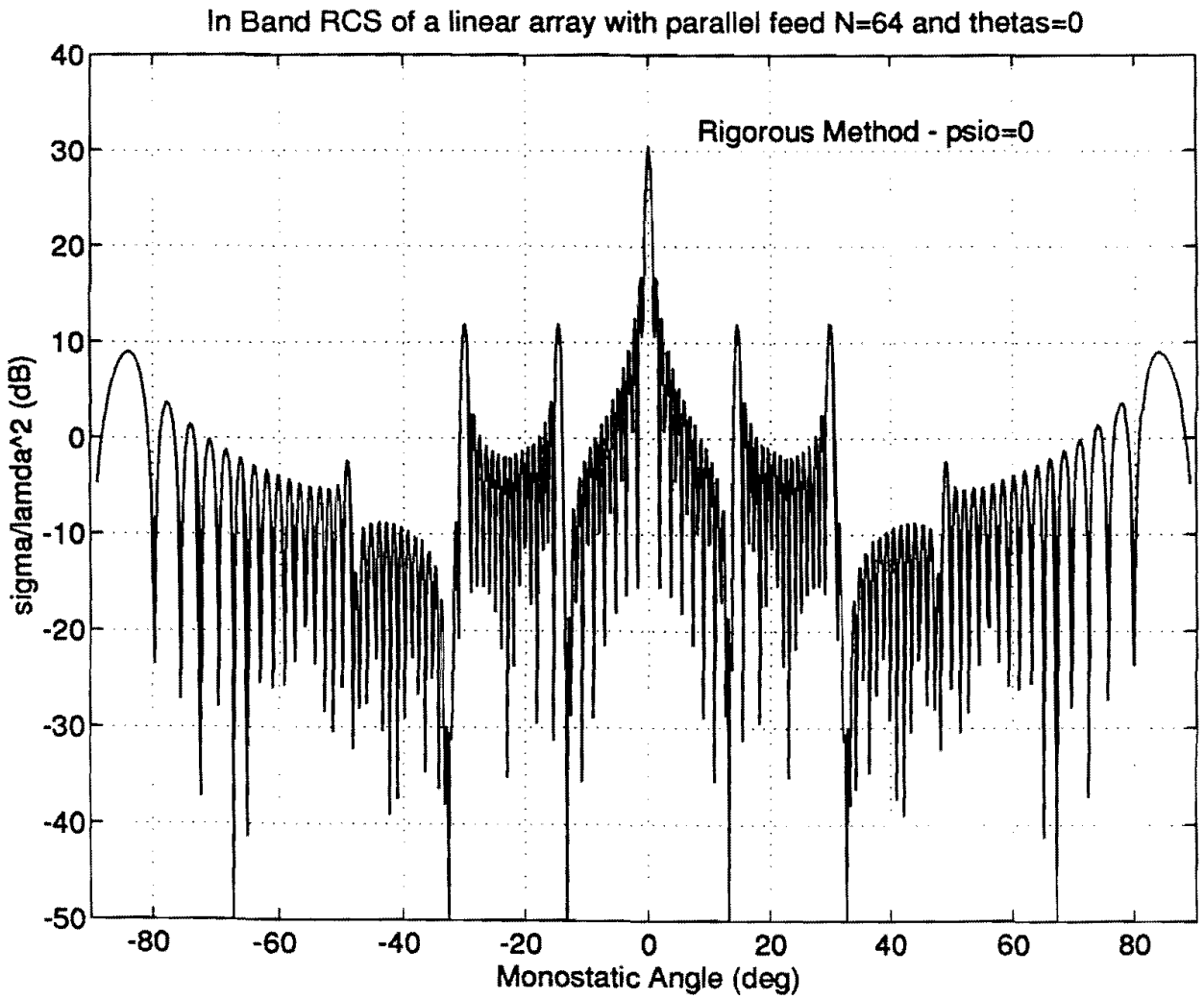

Figure 17. Inband RCS of a Linear Array with a Parallel Feed for N = 64, $\theta_s = 0°$, $\psi_0 = 0$ (Rigorous Method).

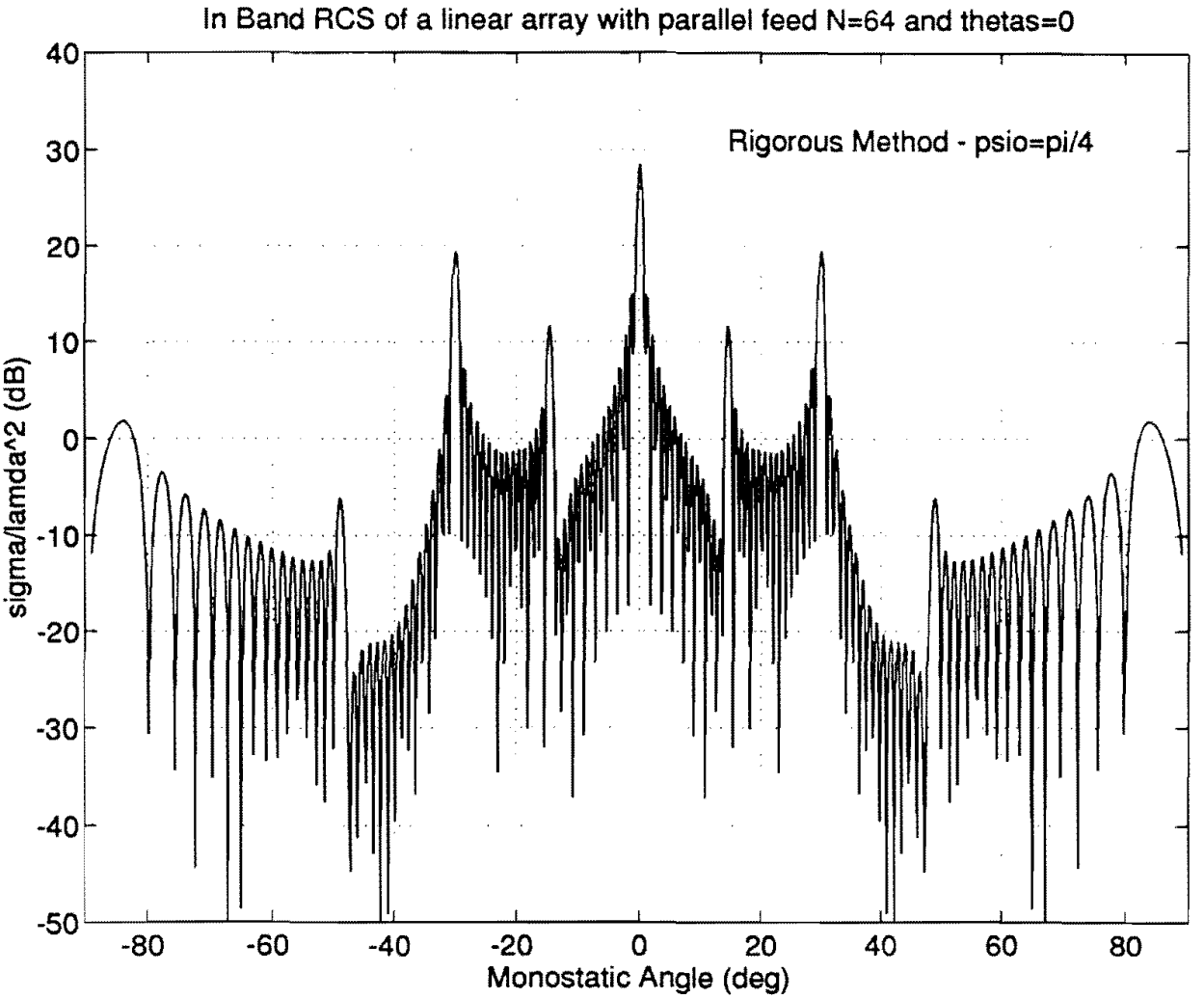

Figure 18. Inband RCS of a Linear Array with a Parallel Feed for N = 64, $\theta_s = 0°$, $\psi_0 = \pi/4$ (Rigorous Method).

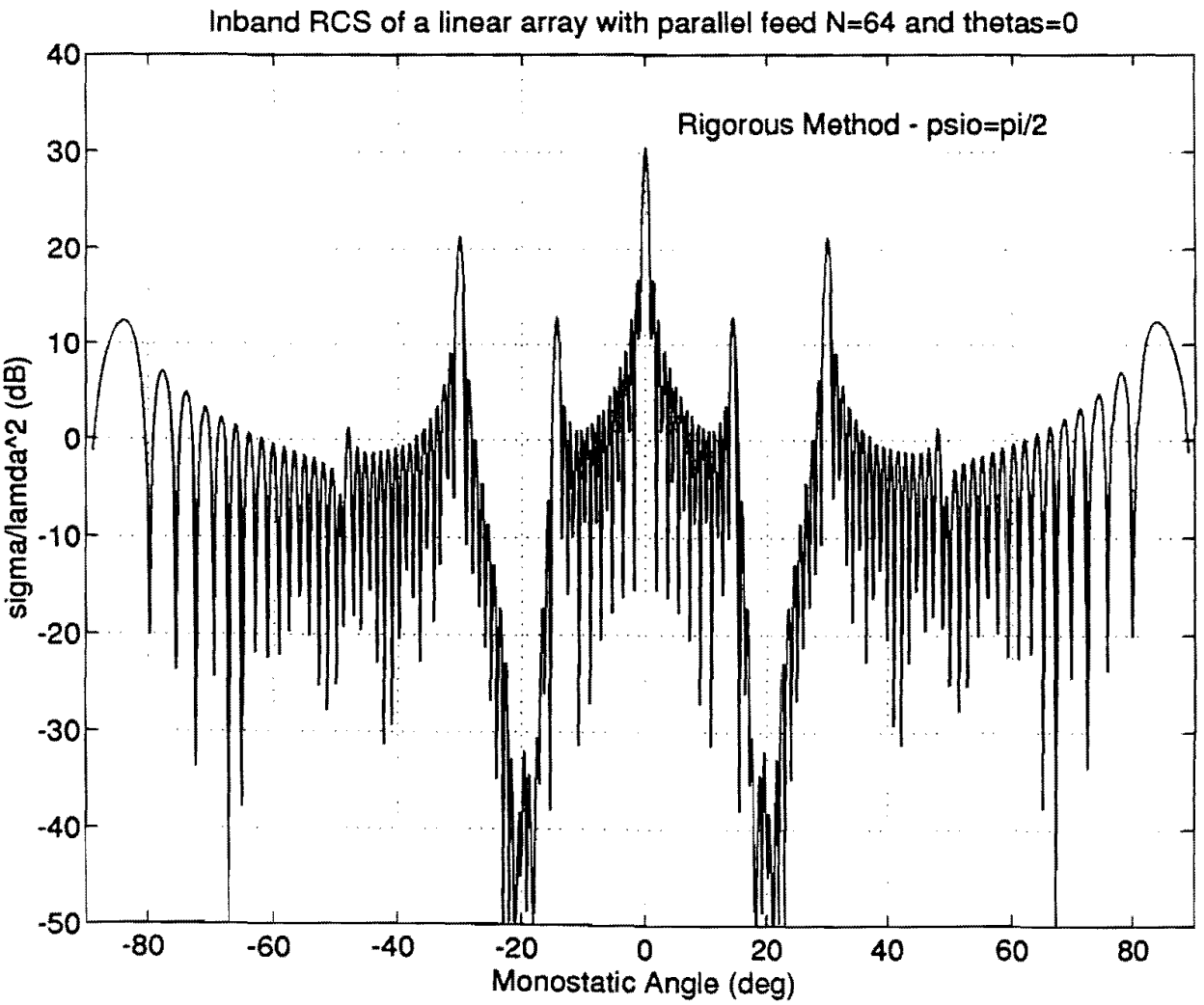

Figure 19. Inband RCS of a Linear Array with a Parallel Feed for N = 64, $\theta_s = 0°$, $\psi_0 = \pi/2$ (Rigorous Method).

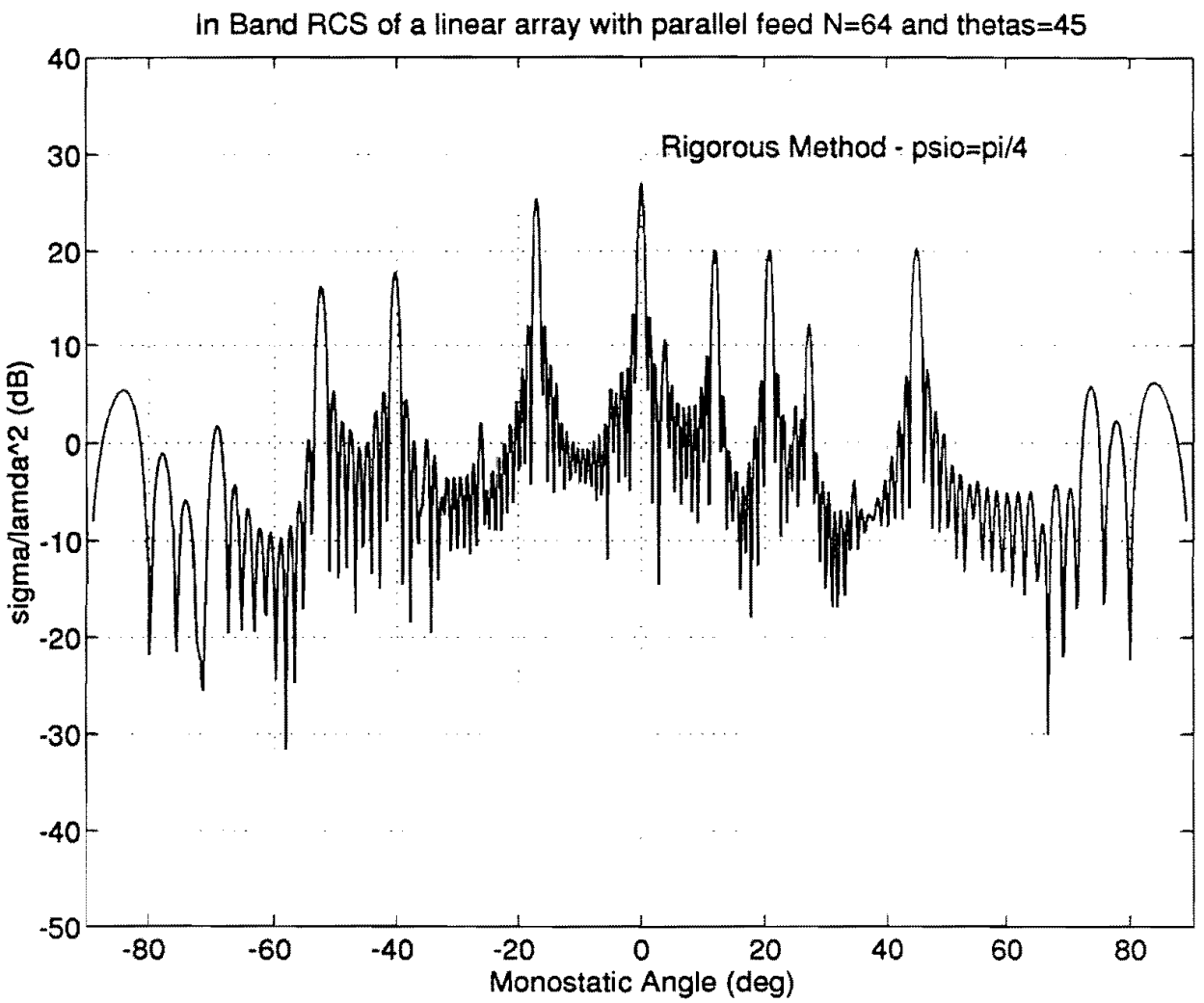

Figure 20. Inband RCS of a Linear Array with a Parallel Feed for N = 64, $\theta_s = 45°$, $\psi_0 = \pi/4$ (Rigorous Method).

cancellation of two scattering contributions. This is not predicted by the approximate method because it sums the individual contributions noncoherently.

C. COMPARISON SUMMARY

The rigorous and approximate results have been presented for broadside and scanned linear arrays. In both cases the specular lobes have almost the same magnitude (within about 1dB) but the coupler lobes vary about 3 dB. This is attributed to the noncoherent summation in the approximation. When the beam is scanned, both methods predict the proper lobe locations, unless complete cancellation occurs.

From a practical point of view, the approximate results are very close to the rigorous. One major difference is the computation times. For $N = 64$, the rigorous method takes about eight times longer than the approximate method and increases dramatically when N increases (for $N = 128$ over 12 times). A more important difference is that if the number of levels of couplers is increased, the scattering equations must be completely rewritten and programmed. For the approximate method, more terms only need to be added to equation (33).

V. CONCLUSIONS

An approximate scattering model for arrays with parallel feed networks has been presented. Calculations for several cases were compared to a rigorous method which includes all the interactions between the feed devices and aperture. The approximate method was in good agreement with the rigorous method in predicting RCS lobe positions, heights, and behavior with scanning.

There are several advantages to the approximate approach. First, it is computationally efficient, allowing two-dimensional contours to be generated in minutes. Second, it can be easily extended to an arbitrary number of elements and coupler levels. The disadvantage is that a noncoherent addition of terms does not predict total cancellation conditions. However, most RCS designers are primarily concerned with the "worst case" conditions for highest RCS, and in this sense the approximate method is sufficient.

Future efforts should be directed at increasing the number of coupler levels, and adding a coupling network in the y dimension of the two-dimensional array. Also, methods of reducing the inband RCS should be investigated.

APPENDIX A

MATLAB PROGRAM FOR LINEAR ARRAYS

```
% Phased arrays
% Written by V.FLOKAS - 22 APR.1994
% Inband RCS of a linear array with parallel feed
clear
clg
thetas=input('Enter scanned angle in degrees thetas= ')
% Scanning at Phis=0
this=thetas*pi/180;
c=3e8;
f=input('Enter operating frequency in Hz, f= ')
lamda=c/f;
k=2*pi/lamda;
d=0.5*lamda;
chi=k*d*sin(this);
theta=linspace(-89,89,660);
thi=theta*pi/180;
alpha=k*d*sin(thi);
jeta=alpha-chi*ones(1,length(alpha));
l=0.5*lamda;
Ae=d*l;
N=input('Enter the number of elements N=  ')
A=N*Ae;
r=0.2;
t=sqrt(1-(r^2));
a1=(sin(N*alpha))./(N*sin(alpha));
h1=find(isnan(a1));
a1(h1)=ones(size(h1));
a2=(sin(N*jeta))./(N*sin(jeta));
h2=find(isnan(a2));
a2(h2)=ones(size(h2));
a3=(sin(N*jeta))./((N/2)*sin(2*jeta));
h3=find(isnan(a3));
a3(h3)=ones(size(h3));
a4=(sin(N*jeta))./((N/4)*sin(4*jeta));
h4=find(isnan(a4));
a4(h4)=ones(size(h4));
sigma=(4*pi*(A/lamda)^2)*((cos(thi)).^2).*((r^2)*(a1.^2)+((r^2)*(t^4)*
      (a1.^2))+((t^8)*(r^2)*(a2.^2))+((t^8)*(r^2)*((cos(jeta/2)).^4).*
```

```
       (a3.^2))+((t^8)*(r^2)*((sin(jeta/2)).^4).*(a3.^2))+
       ((t^8)*(r^2)*((cos(jeta/2)).^4).*((cos(jeta)).^4).*(a4.^2))+
       ((t^8)*(r^2)*((cos(jeta/2)).^4).*((sin(jeta)).^4).*(a4.^2)));
sig=10*log10(sigma/(lamda^2));
figure(1)
plot(theta,sig),grid
xlabel('Monostatic Angle (deg)')
ylabel('sigma/lamda^2  (dB)')
title(['In Band RCS of a linear array with parallel feed  N= ',num2str(N),'
and thetas=',num2str(thetas), ])
gtext('Approximate Method')
axis([-90 90 -50 40])
pause
sec=(4*pi*(A/lamda)^2)*((cos(thi)).^2).*(((t^8)*(r^2)*((cos(jeta/2)).^4).*
((cos(jeta)).^4).*(a4.^2))+((t^8)*(r^2)*((cos(jeta/2)).^4).*((sin(jeta)).^4).
       *(a4.^2)));
s=10*log10(sec/(lamda^2));
figure(2)
plot(theta,s),grid,xlabel('Monostatic Angle (deg)'),ylabel('sigma/lamda^2
 (dB)')
title(['In Band RCS of a linear array with Parallel feed N= ',num2str(N),'
      and thetas=',num2str(thetas), ])
gtext('Second level of couplers')
axis([-90 90 -50 40])
pause
fir=(4*pi*(A/lamda)^2)*((cos(thi)).^2).*((t^8)*(r^2)*((cos(jeta/2)).^4).*
    ((cos(jeta)).^4).*(a4.^2))+
     ((t^8)*(r^2)*((cos(jeta/2)).^4).*((sin(jeta).^4).*(a4.^2)));
s1=10*log10(fir/(lamda^2));
figure(3)
plot(theta,s1),grid,xlabel('Monostatic Angle (deg)'),ylabel('sigma/lamda^2
 (dB)')
title(['In Band RCS of a linear array with parallel feed N= ',num2str(N),'
      and thetas=',num2str(thetas), ])
gtext('First level of couplers')
axis([-90 90 -50 40])
```

APPENDIX B

MATLAB PROGRAM FOR PLANAR ARRAYS

```
% Phased arrays
% Written by V.FLOKAS - 22 APR.1994
% Part (a) - Linear plot for 2-d array
clear
clg
thetas=input('Enter scanned angle in degrees thetas=  ')
this=thetas*pi/180;
Phis=input('Enter scanned angle in degrees Phis= ')
phis=Phis*pi/180;
c=3e8;
f=input('Enter operating frequency in Hz=  ')
lamda=c/f;
k=2*pi/lamda;
dx=0.5*lamda;
dy=dx;
chiox=k*dx*sin(this)*cos(phis);
chioy=k*dy*sin(this)*sin(phis);
theta=linspace(-89,89,460);
thi=theta*pi/180;
PHI=Phis;       % IN MONOSTATIC RCS (PHI CUT = PHI SCANNED)
phi=PHI*pi/180;
u=sin(thi).*(ones(1,length(thi))*cos(phi));
v=sin(thi).*(ones(1,length(thi))*sin(phi));
alpha=k*dx*u;
beta=k*dy*v;
jetax=alpha-chiox*ones(1,length(alpha));
jetay=beta-chioy*ones(1,length(beta));
l=0.5*lamda;
Nx=input('Enter the number of elements Nx=  ')
Ny=Nx;
A=Nx*Ny*dx*dy;
r=0.2;
t=sqrt(1-(r^2));
a1=(sin(Nx*alpha))./(Nx*sin(alpha));
h1=find(isnan(a1));
a1(h1)=ones(size(h1));
a2=(sin(Nx*jetax))./(Nx*sin(jetax));
h2=find(isnan(a2));
```

```
a2(h2)=ones(size(h2));
a3=(sin(Nx*jetax))./((Nx/2)*sin(2*jetax));
h3=find(isnan(a3));
a3(h3)=ones(size(h3));
a4=(sin(Ny*beta))./(Ny*sin(beta));
h4=find(isnan(a4));
a4(h4)=ones(size(h4));
a5=(sin(Ny*jetay))./(Ny*sin(jetay));
h5=find(isnan(a5));
a5(h5)=ones(size(h5));
a6=(sin(Nx*jetax))./((Nx/4)*sin(4*jetax));
h6=find(isnan(a6));
a6(h6)=ones(size(h6));
sigma=(4*pi*(A/lamda)^2)*((cos(thi)).^2).*((r^2)*((a1.*a4).^2)+((r^2)*
(t^4)*((a1.*a4).^2))+((t^8)*(r^2)*((a2.*a5).^2))+((t^8)*(r^2)*
          ((cos(jetax/2)).^4).*
  ((a3.*a5).^2))+((t^8)*(r^2)*((sin(jetax/2)).^4).*((a3.*a5).^2))+
   ((t^8)*(r^2)*((cos(jetax/2)).^4).*((cos(jetax)).^4).*((a6.*a5).^2))+
    ((t^8)*(r^2)*((cos(jetax/2)).^4).*((sin(jetax)).^4).*((a6.*a5).^2)));
sig=10*log10(sigma/(lamda^2));
% Contribution from first level of couplers (sum and difference arms)
sigma1=(4*pi*(A/lamda)^2)*((cos(thi)).^2).*(((t^8)*(r^2)*
          ((cos(jetax/2)).^4).
        *((a3.*a5).^2))+((t^8)*(r^2)*((sin(jetax/2)).^4).*((a3.*a5).^2)));
 sig1=10*log10(sigma1/(lamda^2));
% Contribution from second level of couplers
sigma2=(4*pi*(A/lamda)^2)*((cos(thi)).^2).*(((t^8)*(r^2)*((cos(jetax/2)).
^4).*((cos(jetax)).^4).*((a6.*a5).^2))+((t^8)*(r^2)*((cos(jetax/2)).^4).
        *((sin(jetax)).^4).*((a6.*a5).^2)));
  sig2=10*log10(sigma2/(lamda^2));
figure(1)
plot(theta,sig),grid
axis([-90 90 -30 80])
xlabel('Monostatic Angle (deg)')
ylabel('sigma/lamda^2  (dB)')
title('In Band RCS of a planar 2-D array with parallel feed')
gtext(['Approximate Method - Nx=',num2str(Nx),'=Ny=N and thetas=',
num2str(thetas)
gtext(['Phis=',num2str(Phis), ])
pause
figure(2)
```

```
plot(theta,sig1),grid
axis([-90 90 -30 80])
xlabel('Monostatic Angle (deg)')
ylabel('sigma/lamda^2  (dB)')
title('In Band RCS of a planar 2-D array with parallel feed -
 First Level of Couplers')
gtext(['Approximate Method - Nx=',num2str(Nx),'=Ny=N and thetas='
,num2str(thetas), ])
gtext(['Phis=',num2str(Phis), ])
pause
figure(3)
plot(theta,sig2),grid
axis([-90 90 -30 80])
xlabel('Monostatic Angle (deg)')
ylabel('sigma/lamda^2  (dB)')
title('In Band RCS of a planar 2-D array with parallel feed -
 Second Level of  Couplers')
gtext(['Approximate Method - Nx=',num2str(Nx),'=Ny=N and thetas=
',num2str(thetas), ])
gtext(['Phis=',num2str(Phis), ])
pause
% Part(b) - Contour plot for the same array
clear thi phi u v
du=0.005;
dv=0.005;
nu=fix(2/du)+1;
nv=fix(2/dv)+1;
 for i=1:nu
    u(i)=-1+(i-1)*du;
   for j=1:nv
     v(j)=-1+(j-1)*dv;
     cc=(u(i))^2+(v(j))^2;
    cth(i,j)=1-((u(i)^2)+(v(j)^2));
 if (cc>1)
     cth(i,j)=0;
 end
    end
 end
[x,y]=meshgrid(u,v);
alpha=k*dx*x;
beta=k*dy*y;
```

```
jetax=alpha-chiox*ones(length(alpha),length(alpha));
jetay=beta-chioy*ones(length(beta),length(beta));
a1=(sin(Nx*alpha))./(Nx*sin(alpha));
 z1=find(isnan(a1));
a1(z1)=ones(size(z1));
a2=(sin(Nx*jetax))./(Nx*sin(jetax));
 z2=find(isnan(a2));
 a2(z2)=ones(size(z2));
a3=(sin(Nx*jetax))./((Nx/2)*sin(2*jetax));
 z3=find(isnan(a3));
 a3(z3)=ones(size(z3));
a4=(sin(Ny*beta))./(Ny*sin(beta));
 z4=find(isnan(a4));
a4(z4)=ones(size(z4));
a5=(sin(Ny*jetay))./(Ny*sin(jetay));
 z5=find(isnan(a5));
 a5(z5)=ones(size(z5));
a6=(sin(Nx*jetax))./((Nx/4)*sin(4*jetax));
 z6=find(isnan(a6));
a6(z6)=ones(size(z6));
q=(4*pi*(A/lamda)^2)*(cth);
n=(r^2)*((a1.*a4).^2)+(r^2)*(t^4)*((a1.*a4).^2)+(t^8)*(r^2)*
((a2.*a5).^2)+(t^8)*(r^2)*((cos(jetax/2)).^4).*
  ((a3.*a5).^2)+(t^8)*(r^2)*((sin(jetax/2)).^4).*((a3.*a5).^2)+
  (t^8)*(r^2)*((cos(jetax/2)).^4).*((cos(jetax)).^4).*((a6.*a5).^2)+
   (t^8)*(r^2)*((cos(jetax/2)).^4).*((sin(jetax)).^4).*((a6.*a5).^2);
sigma=q.*n;
sigma=abs(sigma);
sig=10*log10((sigma/(lamda^2))+eps*ones(length(sigma),length(sigma)));
lev=[80 20];
figure(4)
axis('square')
contour(sig,lev,u,v),grid
axis('square')
xlabel('u'),ylabel('v')
title('In Band RCS of a two-dimensional array - Contour plot')
gtext(['Approximate Method Nx=',num2str(Nx),'=Ny=N and thetas='
,num2str(thetas),]
       gtext(['Phis=',num2str(Phis), ])
```

LIST OF REFERENCES

1. Hansen, R. C., "Relationships Between Antennas as Scatterers and as Radiators," *Proc. IEEE*, Vol. 77, pp. 659-662, May 1989.

2. Montgomery, C. G., R. H. Dicke, and E. M. Purcell, *Principles of Microwave Circuits*, in Radiation Laboratory Series, Vol. 8, pp. 317-333, New York, McGraw-Hill, 1968.

3. Kahn, W. K., and H. Kurss, "Minimum Scattering Antennas," *IEEE Trans. on Antennas and Propagation*, Vol. AP-13, pp. 671-675, September 1965.

4. Green, R. B., "Scattering from Conjugate Matched Antennas," *IEEE Trans. Antennas and Propagation*, Vol. AP-14, pp. 17, January 1966.

5. Jenn, D. C., *Radar Cross Section Engineering*, in publication, AIAA Press.

6. Jenn, D. C., "A Complete Matrix Solution for Antenna Analysis," *IEEE International Symposium Digest*, Vol. 1, AP-S, pp. 126-129, June 1989.

INITIAL DISTRIBUTION LIST

		No. Copies
1.	Defense Technical Information Center Cameron Station Alexandria, Virginia 22304-6145	2
2.	Library, Code 52 Naval Postgraduate School Monterey, California 93943-5101	2
3.	Chairman, Code EC Department of Elactrical and Computer Engineering Naval Postgraduate School Monterey, California 93943-5121	1
4.	Prof. David C. Jenn, Code EC/ Jn Department of Electrical and Computer Engineering Naval Postgraduate School Monterey, California 93943-5121	2
5.	Prof. Ramakrishna Janaswamy, Code EC/Js Department of Electrical and Computer Engineering Naval Postgraduate School Monterey, California 93943-5121	1
6.	Prof. Phillip E.Pace, Code EC/Pc Department of Electrical and Computer Engineering Naval Postgraduate School Monterey, California 93943-5121	1
7.	Embassy of Greece Naval Attache 2228 Massachusetts Ave, NW Washington, DC 20008	2
8.	LTJG Vassilios Flokas, Hellenic Navy 1, Iofontos St. 11634, Athens Greece	3